TITLE

Some like it hot: efficiency of the Type 3 Secretion System and activation of plant defenses have multiple thermosensitive behaviors in the *Pseudomonas syringae* complex

AUTHORS

E. Caullireau[1,2], D. Danzi[1], V.M. Tempo[1], M. Pandolfo[1], C.E. Morris[2], E. Vandelle[1]

Corresponding author: elodiegenevieve.vandelle@univr.it

AFFILIATIONS

[1] Department of Biotechnology, University of Verona, Strada Le Grazie 15, 37134 Verona, Italy.

[2] Plant Pathology, INRAE, 84140 Montfavet, France.

ABSTRACT

The *Pseudomonas syringae* species complex is a very important plant pathogenic bacterium, causing damage and economic losses on many crops. Research efforts for the understanding of the determinants of the host-range of a given strain are considerable. Recently, we showed that the inability of a *P. syringae* pv. *actinidiae* strain to trigger ETI in *A. thaliana* is due to an inefficient T3SS and not to the absence of a recognized effector. In this context, we compared several *P. syringae* strains belonging to different phylogroups and carrying the same plasmid-born avirulence gene for their ability to induce an HR in *A. thaliana* Col-0, as a marker of T3SS efficiency. *Pto* DC3000 *AvrB* and *Pma* M6 *AvrB* consistently triggered a strong HR while other strains induced it at different intensities significantly depending on temperature. Both behaviors of low and warm temperature-dependency for T3SS efficiency were observed among thermosensitive strains, irrespective of their *in-vitro* growth optimum. Surprisingly,

differences were also observed among quasi-clonal strains. These results reveal a strongly strain-specific regulatory role of temperature in effector injection and reinforce the notion that the presence/absence of effectors is not sufficient to predict the outcome of plant-bacteria interactions. Moreover, this work highlights the necessity to study bacterial virulence in a broader set of strains insofar as *Pto* DC3000 is a reliable model strain but not representative of the *P. syringae* complex.

FUNDING

The doctoral grant of E.C. was funded by the Italian Ministry of Education, Universities and Research.

35 **INTRODUCTION**

36 *Pseudomonas syringae* is a gram-negative bacterium that poses a threat to global agricultural
37 production with new outbreaks that emerge regularly (Lamichhane *et al.*, 2014, 2015). *P.*
38 *syringae* has been divided into 13 phylogenetic groups (phylogroups, PG), further divided into
39 23 clades (Berge *et al.*, 2014). During the infection process, *P. syringae* relies on an arsenal of
40 secreted virulence factors, such as secretion systems, quorum sensing (QS), production of
41 phytotoxins (coronatine, syringomycin…), hormones, exopolysaccharides (EPS), siderophores
42 etc. (Melotto & Kunkel, 2013; Sharma *et al.*, 2023). *P. syringae* pathogenesis is predominantly
43 mediated by the type III secretion system (T3SS), a highly conserved needle-like specialized
44 protein secretion machinery, found in numerous gram-negative bacterial pathogens affecting
45 plants and animals. T3SS forms a continuous channel, guiding the translocation of diverse
46 proteinaceous effectors (T3SEs) from the bacterium directly into the host cell or apoplast
47 (Roine *et al.*, 1997; Jin & He, 2001; Li, 2002; Büttner & He, 2009). T3SEs facilitate the invasion
48 of plant host cells, suppress plant immunity, or interfere with essential plant cellular processes
49 (Lee, 1997; Mudgett & Staskawicz, 1998; Hueck, 1998; Galán & Collmer, 1999; Cunnac *et al.*,
50 2009; Guo *et al.*, 2009). *P. syringae* strains in the phylogroups with the canonical T3SS
51 commonly harbor a repertoire of approximately 15-30 T3SEs, playing distinct roles within the
52 host plant (Guttman *et al.*, 2002; Chang *et al.*, 2005; Lindeberg *et al.*, 2012; Xin *et al.*, 2016,
53 2018; Martel *et al.*, 2022). Of note, there is no direct relationship between the size or content
54 of the T3SE repertoire and host range (Baltrus *et al.*, 2017; Morris *et al.*, 2019). When
55 considered individually, numerous T3SEs are dispensable for *P. syringae* virulence. However,
56 collectively, they redundantly contribute to disarming plant immunity (Lindeberg *et al.*, 2012;
57 Ruiz-Bedoya *et al.*, 2023).

58 Throughout their co-evolution with pathogens, plants have evolved an extensive array of
59 defenses to recognize them and block pathogenesis. Common bacterial features such as
60 flagellin, lipopolysaccharide (LPS), peptidoglycan and elongation factor Tu (EF-Tu) contain
61 conserved molecular motifs (Pathogen or Microbe-Associated Molecular Patterns; P/MAMPs)
62 that are sensed by the plant as non-self, through their binding to Pattern Recognition
63 Receptors (PRRs) situated on the plant cell surface (Boller & Felix, 2009; Cui *et al.*, 2009). Non-
64 self detection by PRRs is the first step of the PTI or MTI, for PAMP-/MAMP-Triggered Immunity,
65 implying then various cellular responses to inhibit pathogen growth and virulence
66 mechanisms, such as T3SS activation for bacterial pathogens (Crabill *et al.*, 2010; Anderson *et*
67 *al.*, 2014). On the other hand, T3SEs serve the primary function of subverting PTI, targeting
68 key signaling components to interfere with their function. In response, plants have evolved
69 cytoplasmic receptors called 'resistance' (R) proteins to detect some of these effectors, either
70 directly or indirectly, leading to the activation of the Effector-Triggered Immunity (ETI)
71 (Thomma *et al.*, 2011). R genes typically encode for NLR proteins (Nucleotide-binding
72 oligomerization domain-Like Receptor), consisting of a nucleotide-binding site (NBS) and a
73 leucine-rich repeat (LRR) domain (Monteiro & Nishimura, 2018). PTI and ETI are unlikely to be
74 separate processes as suggested in the 'zigzag' model (Jones & Dangl, 2006), but both non-self
75 and virulence effector recognition by membrane and cytoplasmic receptors are simultaneously
76 involved in a global surveillance system to respond effectively to pathogen attack (Ngou *et al.*,
77 2021; Yuan *et al.*, 2021). ETI is a potentiation of PTI, often leading to rapid and localized
78 programmed cell death, known as the hypersensitive response (HR). HR generally occurs
79 within 2 to 6 hours post initial host-pathogen contact, inhibiting the propagation of (hemi)-
80 biotrophic pathogens, such as *P. syringae* (Coll *et al.*, 2011; Balint-Kurti, 2019).

81 According to the 'disease triangle' paradigm (Stevens, 1960), plant diseases arise from the
82 interplay between a susceptible plant and a virulent pathogen, under conducive
83 environmental conditions, resulting in a compatible reaction. Overall plant-pathogen
84 interaction mechanisms are highly influenced by environmental conditions, which can either
85 favor, have neutral effects, or hinder both partners (Velásquez *et al.*, 2018; Xin *et al.*, 2018).
86 Among the environmental factors, temperature has a regulatory role of virulence in plant-
87 associated bacteria (reviewed in Smirnova *et al.*, 2001; Velásquez *et al.*, 2018).
88 Within the *P. syringae* species complex, temperature variations impact various traits crucial for
89 bacterial fitness, including phytotoxins, EPS biosynthesis, motility or quorum-sensing (Nüske
90 & Fritsche, 1989; Palmer & Bender, 1993; Peñaloza-Vázquez *et al.*, 1997; Bender *et al.*, 1999;
91 Ullrich *et al.*, 2000; Smirnova *et al.*, 2001; Weingart *et al.*, 2004; Li *et al.*, 2006; Aguilera *et al.*,
92 2007, 2017; Braun *et al.*, 2009; Hockett *et al.*, 2013; Arvizu-Gómez *et al.*, 2013a; Scalschi *et al.*,
93 2022; Krishna *et al.*, 2022). T3SS has also been investigated concerning its possible
94 thermoregulation. In *P. syringae* pv. *syringae* and pv. *tomato* DC3000, the *in-vitro* secretion of
95 HopPsyA and AvrPto effectors was impaired at temperatures above 22°C and 20°C, indicating
96 some kind of low-temperature dependency for their T3SS efficiency (Van Dijk *et al.*, 1999). In
97 contrast, recent findings in strain DC3000 revealed that the translocation of T3SEs in *A.*
98 *thaliana* cells is enhanced at 30°C compared to 23°C, indicating the possible T3SS efficiency
99 even at elevated temperatures (Huot *et al.*, 2017). However, in tomato, the expression of T3SS-
100 related genes *hrpL* and *hrpA* in this same strain was not affected by a temperature rise from
101 26°C to 31°C, although the expression of the avirulence gene *AvrPtoB* was significantly reduced
102 (Scalschi *et al.*, 2022). On the other hand, for *P. syringae* pv. *actinidiae* strains, it was shown
103 that there was no difference in *hrpA1* promoter activity *in vitro* across a temperature range of
104 18-28°C, nonetheless, substantial differences were evident at a functional level, demonstrating

105 a low-temperature dependency for T3SS efficiency for these strains (Puttilli *et al.*, 2022).
106 However, the complete implications of warm temperatures on *P. syringae* virulence in plants
107 remain poorly understood (Li *et al.*, 2006; Hockett *et al.*, 2013). Studies indicate complex
108 interactions with plant immune signaling pathways, emphasizing the need for further research
109 to understand their implications in terms of disease (Cheng *et al.*, 2013; Huot *et al.*, 2017).
110 Thermosensing principles in phytopathogens are less understood than those of pathogens of
111 warm-blooded organisms. They were assumed to be different, given the ecological differences
112 between these groups of pathogens (Smirnova *et al.*, 2001; Klinkert & Narberhaus, 2009).
113 Nevertheless, some common mechanisms have been identified in both plant- and mammal-
114 associated bacteria. Various molecular strategies are involved in sensing temperature, such as
115 two-component systems (TCSs) that typically involve a membrane-bound sensor histidine
116 kinase that detects environmental stimuli and a cytoplasmic response regulator influencing
117 gene expression upon phosphorylation of an aspartic acid (Klinkert & Narberhaus, 2009).
118 Several TCS were shown to be involved in the thermoregulation of virulence mechanisms, such
119 as the VirA/G system in *Agrobacterium tumefaciens* (Jin *et al.*, 1993), the GacS/GacA system
120 in *P. syringae* pv. *phaseolicola* (Arvizu-Gómez *et al.*, 2013b; Tribelli & López, 2022) and the
121 CorRSP system in *P. syringae* pv. *glycinea* (Ullrich *et al.*, 1995).
122 Evidence of the influence of temperature in regulating virulence factors in *P. syringae* species
123 complex has been documented, however, there have not been studies dedicated to comparing
124 strains under identical conditions. Consequently, we wanted to further understand the role of
125 the temperature on the function/activation dynamics of the T3SS, investigating a broader
126 range of diversity within the *P. syringae* species complex under comparable conditions. For this
127 purpose, we transformed 13 strains of *P. syringae* to carry the effector AvrB and infiltrated
128 them into *Arabidopsis thaliana* Col-0 leaf disks. In this model plant, AvrB is indirectly

129 recognized by the resistance protein RPM1, through RIN4 modification, which triggers HR
130 (Innes *et al.*, 1993; Mackey *et al.*, 2002; Mudgett, 2005). Infiltrated leaf disks were incubated
131 at different temperatures and the quantification of electrolyte leakage served as the indicator
132 of HR onset. Conductivity increase was used as a proxy for T3SS efficiency, and this allowed us
133 to effectively discriminate strains based on a robust phenotype directly linked to the activation
134 of the T3SS. Based on the different behaviors we observed in response to temperature, we
135 investigated the genomes of the strains in an attempt to decipher the origin of the
136 thermosensing mechanisms.

137 **MATERIAL & METHODS**

138

139 **Bacterial strains and culture conditions**

140 Thirteen *Pseudomonas syringae* strains were selected for this study (**Tab. 1**). These strains
141 represented four phylogroups/clades (1a, 1b, 2d, and 3a). The geographical origin and isolation
142 source of the strains varied, encompassing annual crops (*e.g.* M6, T1) (Whalen *et al.*, 1991;
143 Debener *et al.*, 1991), woody plants (*e.g.* J35, CRA-FRU 8.43, MAFF302273) (Takikawa *et al.*,
144 1989; Sawada *et al.*, 1999; Ferrante & Scortichini, 2010), and environmental reservoirs like
145 rivers or snow (*e.g.* LAB0041, USA007) (Morris *et al.*, 2010; Berge *et al.*, 2014). Genomic
146 relatedness within a phylogroup was also considered, aiming for a balance of very divergent
147 and closely related strains, such as the three 'CC' strains (CC0073, CC0094, and CC1498) that
148 are quasi-clones (Morris *et al.*, 2000, 2008; Monteil *et al.*, 2016). Model strains DC3000, B728a
149 and 1448A were also included in the set as there is a plethora of information about their
150 biology (Cuppels, 1986; Loper & Lindow, 1987; Taylor *et al.*, 1996).

151 Wild-type (WT) *P. syringae* strains were grown at 28°C on King's B agar (KB) (King *et al.*, 1954)
152 – supplemented with rifampicin at 50µg/mL for DC3000 and B728a strains. Kanamycin at
153 50µg/mL was added for the culture of *AvrB* mutants. Single colonies of each strain were picked
154 and grown overnight in liquid KB medium – supplemented with rifampicin at 50µg/mL for
155 DC3000 and B728a strains and with kanamycin at 50µg/mL for *AvrB* mutants, with agitation at
156 190rpm at 28°C.

157

158 ***AvrB*-transformation**

159 Four mL of fresh WT bacterial suspension were centrifuged (5min at 4500g at 4°C) and pellets
160 were washed three times in 1mL and then resuspended in 30-50µL of sterile glycerol 10%

161 solution kept on ice. Once the pure plasmid carrying *AvrB* gene (pVB01 Km^R; Innes *et al.*, 1993)
162 was added to the suspensions, they underwent then an electroporation process. Once
163 recovered, the suspensions were streaked on petri dishes containing KB agar – supplemented
164 with kanamycin at 50µg/mL for all strains plus rifampicin at 50µg/mL for DC3000 and B728a
165 strains. Plates were incubated for 48 up to 72 hours a 28°C. Mutant colonies were picked and
166 *AvrB* presence was checked by PCR using Promega GoTaq™ DNA polymerase (Fisher Scientific,
167 USA) and specific primers (FOR: ATGGGCTGCGTCTCGTCAAAAAGCA, REV:
168 TTAAAAGCAATCAGAATCTAGCAAG, annealing temperature= 65°C) followed by electrophoresis
169 of the amplicons on a 1-1.5% (w/v) agarose gel.
170
171 ***AvrB* expression control**
172 Relative expression levels of *AvrB* among the mutant strains were evaluated by real-time PCR.
173 Four mL of fresh suspension of *AvrB*-transformed *P. syringae* strains grown overnight in
174 selective medium were centrifuged (5min at 4500g at room temperature) and total RNA was
175 extracted from bacterial pellets using TRIzol substitute (EuroGold TriFast™ Kit, EuroClone,
176 Italy) according to manufacturer instructions. Extraction yield and quality of the transcripts
177 were checked by spectrophotometric reading (NanoDrop™, Thermo Fisher Scientific, USA).
178 Samples with absorbance ratios A_{260nm}/A_{230nm} or A_{260nm}/A_{280nm} outside the range of [2 ± 0.5]
179 were cleaned following a lithium chloride RNA precipitation treatment (solution made of 7.5M
180 LiCl, 50mM EDTA, pH 8.0). 1-2µg RNA per sample underwent DNase treatment (TURBO™
181 DNase, Life Technologies, USA) then the single-stranded complementary DNA synthesis was
182 performed from 0.5-1µg of template RNA using SuperScript™ III Reverse Transcriptase enzyme
183 (Invitrogen, USA) according to manufacturer instructions. Samples get 10-fold diluted and
184 procedure was performed using Luna® Universal qPCR Master Mix (New England Biolabs, USA)

185 and *rpoD* housekeeping gene as reference, and amplification was run on a QuantStudio™ 3
186 real-time PCR system (Applied Biosystems, USA) (primers *AvrB* FOR: ATACTCTGCATTCGCCTCCG,
187 REV: TCAACGACTCTGGCAAGGAC; primers *rpoD* FOR: AACTTGCGTCTGGTGATCTC, REV:
188 ATCAAGCCGATGTTGCCTTC). *AvrB* expression was determined using the $2^{-\Delta\Delta Ct}$ method and
189 normalized against *rpoD*, and fold-induction for each strain was established relative to the
190 strain DC3000 *AvrB.*
191
192 **Ion-leakage experiments**
193 Hypersensitive response (HR) induction in *Arabidopsis thaliana* Col-0 was assessed by
194 quantifying programmed cell death through ion-leakage measurement, as previously
195 published (Johansson *et al.*, 2015; Imanifard *et al.*, 2018) with slight modifications. *A. thaliana*
196 Col-0 plants were cultivated in a mixture of peat soil and perlite (4/1, v/v) in a growth chamber
197 set at 24°C/21.5°C thermoperiod and 8 h light–16 h dark photoperiod with 70% of relative
198 humidity for 6 to 8 weeks. Three healthy plants with six 5-mm leaf disks detached from a same
199 plant with a cork borer were used for each experimental condition. To recognize the plant they
200 were detached from, leaf disks were marked with a colored felt-tip and were then transferred
201 into a 50mL tube containing $MgCl_2$ 10mM solution while bacterial suspension preparation. Ten
202 mL of fresh suspension of *AvrB*-expressing *P. syringae* strains grown overnight in selective
203 medium were centrifuged (5min at 4500g at room temperature) and pellets were washed
204 three times in 10mL of sterile $MgCl_2$ 10mM solution. Optical density at 600nm was measured
205 by spectrophotometer (Evolution™, ThermoFisher Scientific, USA) and bacterial cells were
206 finally resuspended in sterile $MgCl_2$ 10mM solution to reach 10^8 CFU/mL (OD_{600nm} = 0.1; final
207 volume = 30mL). Leaf disks were infiltrated with the bacterial suspensions using a 50mL syringe
208 or a vacuum chamber. Sterile $MgCl_2$ 10mM solution or *hrp*-inducing medium (HIM; using

209 glycerol 27mM as carbon source; pH 5.5) (Huynh *et al.*, 1989) were used as negative controls.
210 Infiltrated leaf disks were rinsed twice for 15m in 40mL of milliQ water under gentle agitation
211 (90 rpm) at room temperature to eliminate suspension/mock solution trace and ions leaked
212 due to mechanical damage. Infiltrated leaf disks were then distributed into 12-well plate
213 containing 2mL of milliQ water per well in order to have: (i) six disks per well, (ii) two disks
214 from each of the three different plants per well, (iii) three identical wells (one plate column)
215 per each experimental modality. Initial conductivity values ($\mu S.cm^{-1}$) in each well was
216 measured prior plates incubation (120rpm; constant light of 80 $\mu mol.m^{-2}.s^{-1}$) at different
217 temperatures (18, 24 and 28°C) using a compact conductometer (LAQUAtwin EC-11, HORIBA
218 Scientific, Japan). Conductivity increase was measured every 1.5-2 hours during the first 8
219 hours of the experiment, and then twice between 18- and 24-hours post-inoculation (hpi),
220 obtaining from 6 to 9 conductivity measures on average per well. Each experimental modality
221 (*i.e.* one specific *AvrB*-transformed strain infiltrated and then incubated at a certain
222 temperature) was reproduced at least three times (at least 3 `biological replicates' or
223 `replicated experiments').
224
225 **Statistical analysis**
226 For each technical replicate, the conductivity value from the first measure was subtracted to
227 values measured at each successive time points for normalization (Puttilli *et al.*, 2022). For
228 each strain-temperature modality within each replicated experiment, conductivity was
229 calculated as the average of the values of the three technical replicates for each time point,
230 and ion-leakage curves over time were established accordingly. Area under each single
231 conductivity progress curve was calculated (AUCPC), as well as variance and mean AUCPC per
232 modality. Moreover, conductivity values corresponding to precisely 6 hpi and 24 hpi were

233 calculated via linear interpolation, and the ratio 6 hpi/24 hpi was used as a dynamic parameter,
234 indicating how fast a given strain induced HR at a given temperature. Comparison of strains
235 with each other based on the 6 hpi/24 hpi conductivity ratio was assessed by analysis of
236 variance (Kruskal-Wallis test) followed by a post-hoc Dunn's test. The same procedure was
237 conducted to compare the three different temperatures regardless of the strain. Data were
238 represented graphically by boxplots.
239 Each single conductivity progress curve constituted from 6 to 9 time points and was considered
240 as one statistical individual (*i.e.*, one iteration) to fit Linear Mixed-effects Models (LMM). This
241 allowed us to account for the important variability among the diverse experimental replicates
242 of a same modality and, most importantly, to consider the entire time course of electrolyte
243 leakage, rather than focusing solely on isolated time points. The mathematical representation
244 of LMM is: $Y = X\beta + Z\upsilon + \varepsilon$; where Y represents the dependent variable (the measured feature,
245 *i.e.* conductivity increase), $X\beta$ stands for the fixed effects (*i.e.* the potential explanatory
246 variables we want to assess the effect on Y), $Z\upsilon$ stands for the random effects (all the unknown
247 parameters that may be responsible for the huge variability among the different replicated
248 experiments and which we are not directly interested to), and ε represents the residual. Using
249 LMM in RStudio, we evaluated (i) the strain effect (*i.e.* if the ion-leakage following *AvrB*-
250 expressing strain infiltration was significantly different from the ion-leakage due to mock
251 treatment infiltration) to categorize each strain as 'HR-inducer' or 'non-inducer' at each of the
252 tested temperatures; and (ii) the temperature effect (*i.e.* if the ion-leakage following *AvrB*-
253 expressing strain infiltration was significantly different as the incubation temperature changed)
254 on the strains considered as HR-inducers at least at two of the tested temperatures. In this
255 way we estimated the values of model parameters and the associated p-values .
256

257 ***In-vitro* HrpZ secretion**

258 Secretion of HrpZ *in vitro* was assessed for each strain used in ion leakage experiments. Twenty
259 mL of fresh suspension of *AvrB*-expressing *P. syringae* strains grown overnight in selective
260 medium were centrifuged (5min at 4500g at room temperature) and pellets were washed
261 three times in 10mL of sterile minimal medium (HIM). Optical density at 600nm was measured
262 with a spectrophotometer (Evolution™, ThermoFisher Scientific, USA) and bacterial cells were
263 resuspended in sterile HIM to reach 7 x 10^8 CFU/mL (OD_{600nm} = 0.7; final volume = 150mL).
264 Suspensions were divided into three portions of 50mL, each was separately incubated at 18°C,
265 24°C and 28°C with agitation at 190rpm. After 5 and 24 hours of incubation, 25mL of each
266 bacterial suspension was sampled and absorbance at 600nm was measured again (Evolution™,
267 ThermoFisher Scientific, USA). Cell-free culture supernatant was obtained by centrifugation
268 and filtration, and proteins of supernatant were then precipitated with trichloroacetic acid
269 (TCA) as previously described (Kobayashi *et al.*, 1997; Flaugnatti & Journet, 2017) with TCA
270 final concentration at 5%.

271 Samples were mixed with loading buffer (DTT 50mM) and run (10 min at 100V; 80 min at 130V)
272 through two 1.5mm sodium dodecyl sulfate-polyacrylamide gel electrophoresis (SDS-PAGE)
273 12%, either loading 25µL of each sample, or adjusting volume to load the supernatant
274 extracted from *ca.* 10^7 cells (OD_{600nm} = 0.6, final volume = 17.5µL). 180kDa-PageRuler™
275 (ThermoFisher Scientific, USA) was used as protein ladder. One gel was used to assess total
276 soluble protein content in each sample and thus confirm the correct loading ratio: after rinsing
277 with milli-Q water, the gel was stained for 20 minutes in Coomassie R-250 staining solution
278 (isoprophyl alcohol 25%, acetid acid 10%, Coomassie R-250 0.05%) and destained with acetic
279 acid 10% until complete removal of the background. The second gel was transferred onto
280 nitrocellulose blotting membrane (GE HealthCare, USA) for Western Blot analysis. The

281 membrane was immersed for one hour at 37°C in a blocking solution made of phosphate-
282 buffered saline solution (PBS) (NaCl 137mM, KCl 2.7mM, Na_2HPO_4 10mM, KH_2PO_4 1.8mM),
283 supplemented with Tween® 20 0.05% and non-fat dry milk 5%. Then, the membrane was
284 probed with the specific primary anti-HrpZ antibody (Alfano *et al.*, 1996), diluted 1:500 in the
285 same blocking solution, and incubated at room temperature for 1h and a half. Following
286 primary antibody incubation, membrane was washed 3 times for 15m in PBS supplemented
287 with Tween® 20 0.05% under gentle agitation in the dark. Then, the membrane was probed
288 for 1h at room temperature in the dark using the conjugated secondary antibody to
289 horseradish peroxidise (Amersham Biosciences, USA), diluted 1:10000 in the same blocking
290 solution. Finally, after three additional washings in PBS (supplemented with Tween® 20 0.05%
291 for the first two), proteins were visualised (Chemidoc™, ThermoFisher Scientific, USA) by
292 enhanced chemiluminescent (ECL) detection (GE HealthCare, USA). Blot pictures were
293 analyzed using ImageLab software (BioRad, USA). The intensity of each band was normalized
294 to the intensity of the 70kDa band from the ladder. When necessary, relative quantity was then
295 normalized to the optical density measured by the end of the incubation period to adjust the
296 results to the number of cells initially present in each sample.
297
298 ***In-vitro* growth measurement**
299 *In-vitro* bacterial growth under different temperatures was assessed for each strain. Four mL
300 of fresh suspension of *AvrB*-expressing *P. syringae* strains grown overnight in selective medium
301 were centrifuged (5min at 4500g at room temperature) and pellets were washed three times
302 in 1mL of fresh liquid KB. Optical density at 600nm was measured by spectrophotometer
303 (Evolution™, ThermoFisher Scientific, USA) and bacterial cells were then resuspended to reach
304 2 x 10^7 CFU/mL (OD_{600nm} = 0.02; final volume = 2mL). Suspensions were aliquoted in a

305 microtiter plate (200µL per well), with 6 technical replicates per strain, and plates were
306 incubated at 18°C, 24°C and 28°C. Liquid KB (supplemented or not with the antibiotics) was
307 used as negative control. Absorbance at 600nm was measured every 1.5-2 hours during the
308 first 8 hours of the experiment, and then two or three times between 18 and 24 hpi, obtaining
309 from 6 to 9 absorbance measures per well. To eliminate unspecific absorbance signals due to
310 the color of KB medium and the antibiotics, the value from the first measure was subtracted
311 from values measured at each successive time points. Absorbance was then calculated as the
312 average of the values of the six technical replicates for each time point, and bacterial growth
313 curves over time were established accordingly. Each strain-temperature modality was
314 reproduced at least twice, except for T1.
315
316 **Genome comparisons**
317 Genomes of the 13 *AvrB*-expressing strains used in ion-leakage experiments were retrieved
318 mostly from public sequence databases (Pseudomonas Genome Database and NCBI); draft
319 genomes of strains LAB0041, CC0073 and CC1498 were provided by Dr. Cindy Morris. To
320 analyze the genomes, a custom bioinformatic pipeline was created, with the help of the
321 Nextflow framework (Di Tommaso *et al.*, 2017). The pipeline was composed of several steps:
322 i) the FastANI tool was used for rapid many-to-many ANI calculation (Jain *et al.*, 2018); ii)
323 BUSCO was used to assess both the genome quality and protein annotations quality (Manni *et*
324 *al.*, 2021); iii) the Prokka pipeline was used for the protein annotation (Seemann, 2014); iv) the
325 EggNog-mapper tool was used for the functional annotation (Cantalapiedra *et al.*, 2021); and
326 v) the Panaroo pipeline was implemented for the creation of a pangenome of the 13 strains
327 (Tonkin-Hill *et al.*, 2020). Then, the Panaroo output table of gene presence/absence was
328 exploited via an R script to produce interactive tables to determine the number of total genes

329 and specific genes per strain. These tables allowed for the selection of genes present in a given

330 strain, and queries could be performed to obtain information for genes shared by strains.

331 **RESULTS**

332

333 **The intensity of HR induction is not strictly reproducible for individual strains.**

334 To evaluate T3SS functionality at different temperatures, *AvrB*-transformed *P. syringae* strains
335 were infiltrated into *A. thaliana* Col-0 leaf disks. As a T3SS-dependent mechanism, HR was
336 quantified by measuring the increase in ion leakage due to dying cells. Conductivity levels
337 measured among the diverse replicated experiments were highly variable. The conductivity
338 value measured at 24 hours post-infection (hpi) for a given modality (*i.e.*, one strain infiltrated
339 and incubated at one temperature) doubled or tripled among replicated experiments (*e.g*.
340 conductivity values ranged from 80 $\mu S.cm^{-1}$ to 226 $\mu S.cm^{-1}$ for strain DC3000 *AvrB* when
341 incubated at 18°C) (**Fig. 1**). This variability is illustrated in **Fig. 2** for the seven replicated
342 experiments for strain USA007 *AvrB* at 18°C (ratio of areas under the curves calculated for the
343 replicated experiments that induced the most and the least = 2.8). Moreover, conductivity
344 showed considerable heteroscedasticity, *i.e.* there was a positive correlation between the
345 mean area under the curves and their variance with Spearman's coefficient = 0.91; $p < 0.05$
346 (**Supplementary Fig. S1**). Four examples of the relationship between variability and mean
347 conductivity are shown in **Fig. 2**. This large variability raised the question of how the HR
348 induction could be quantified to compare the strains, as addressed in the next section.

349

350 **Intensity of HR induction varies among strains.**

351 To compare HR induction intensity among strains, we accounted for the variability described
352 above by fitting Linear Mixed effects Models to our data. This statistical approach allowed us
353 to classify strains as inducers or non-inducers at each of the temperatures that we tested. This
354 revealed that almost all the *P. syringae* strains induced HR except for J35 *AvrB* at all the

355 temperatures, MAFF302273 *AvrB* at 24°C and 28°C, B728a *AvrB* at 24°C, and 1448A and CRA-
356 FRU 8.43 at 28°C (**Tab. 2**). The inducer strains led to conductivity levels that were significantly
357 greater than those measured in the mock treatment (MgCl2 10mM or *hrp*-inducing medium
358 HIM) ($p < 0.05$) according to Linear Mixed-effects Models. More specifically, our results
359 demonstrated that all the inducer strains varied in the intensity of the HR induction they
360 caused. The model estimated the mean difference in points of conductivity measured between
361 the tested modality and the mock treatment. The values presented in **Tab. 2** ("Estimate") are
362 proxies of the intensity of HR induction for each strain. DC3000 *AvrB* and M6 *AvrB* displayed
363 the highest values ("Estimate" > 65 regardless of the temperature tested), whereas some
364 others such as the three quasi-clonal strains CC0073 *AvrB*, CC0094 *AvrB* and CC1498 *AvrB*
365 averaged less than 20. These differences are also reflected in the mean areas under
366 conductivity progress curves (AUCPC) at each temperature as shown in **Fig. 3**. This proxy of the
367 HR induction intensity was correlated neither with the *AvrB* expression levels (**Supplementary**
368 **Fig. S2**) nor with the bacterial growth capacity at a given temperature (**Supplementary Fig.**
369 **S3**).
370
371 **Intensity of HR induction is temperature-sensitive in half of the inducer strains.**
372 With Linear Mixed-effects Models, we categorized the HR inducer strains according to the
373 temperature-sensitivity of HR induction. Six out of eleven strains were insensitive to a change
374 in temperature (DC3000 *AvrB*, M6 *AvrB*, LAB0041 *AvrB*, CC0073 *AvrB*, 1448A *AvrB*) ($p > 0.05$)
375 (**Tab. 2**). The other HR inducer strains were considered temperature-sensitive ($p < 0.05$) and
376 could be categorized into two groups according to whether the "Estimate" values were
377 negative or positive. In one group, strains showed higher conductivity with lower temperatures
378 (T1 *AvrB*, CRA-FRU 8.43 *AvrB* and USA007 *AvrB*). In the case of CRA-FRU 8.43 *AvrB* strain, the

379 decrease in conductivity observed with increasing temperature led the strain to be categorized
380 as a non-inducer at 28°C (**Tab. 2**). In the other group, strains showed higher conductivity with
381 higher temperatures (CC0094 *AvrB*, CC1498 *AvrB* and B728a *AvrB*). Temperature-sensitivity of
382 the *AvrB*-transformed strains was further confirmed by the analysis of HrpZ secretion *in vitro*
383 as an assessment of T3SS functionality. Interestingly, the strain MAFF302273 *AvrB* displayed a
384 functional T3SS, while it constantly did not lead to conductivity increase once infiltrated into
385 leaf disks, suggesting T3SS inactivation in *A. thaliana* (**Supplementary Fig. S4**).
386
387 **Temperature responsiveness patterns vary among strains but remain consistent within the**
388 **same phylogroup.**
389 A given phylogroup could contain strains that induced HR in temperature-sensitive and
390 temperature-insensitive ways (**Tab. 2**). However, temperature-sensitive strains within a same
391 phylogroup showed the same trend relative to increasing temperature. Indeed, the group of
392 strains whose T3SS was more efficient at the cooler temperatures (*i.e.*, low-temperature-
393 dependent; T1 *AvrB*, CRA-FRU 8.43 *AvrB* and USA007 *AvrB*) and the group whose T3SS was
394 more efficient at warmer temperatures (*i.e.*, warm-temperature-dependent; CC0094 *AvrB*,
395 CC1498 *AvrB* and B728a *AvrB*) belong to the phylogroups 1 and 2d, respectively (**Tab. 2**).
396 Additionally, HrpZ secretion by MAFF302273 *AvrB* was more important as the temperature
397 rose, revealing a pattern of warm-temperature dependency for T3SS efficiency, similar to the
398 other thermosensitive strains belonging to the same phylogroup 2d (**Supplementary Fig. S4**).
399 Nevertheless, dramatic differences among strains even very closely related phylogenetically
400 were still observed, as illustrated by the three quasi-clonal *AvrB*-transformed strains from
401 phylogroup 2d, CC0073, CC0094 and CC1498 (**Tab. 2**) (**Fig. 4**). CC0073 *AvrB* was temperature-
402 independent in its ability to induce HR while CC0094 *AvrB* and CC1498 *AvrB* both showed

403 clearly greater capacity at warmer temperatures. Moreover, in terms of intensity, CC1498 *AvrB*
404 led to higher values of conductivity measured at 24 hpi than CC0073 *AvrB* and CC0094 *AvrB*.
405 Finally, in terms of kinetics, CC0073 *AvrB* was responsible for a faster HR induction at the
406 beginning of the interaction – no matter the temperature concerned – that stalled, whereas
407 CC0094 *AvrB* and CC1498 *AvrB* were much slower in inducing HR (**Fig. 4**).
408
409 **Strains from the *P. syringae* complex display diverse speeds of HR induction.**
410 To account for dynamic aspects in the behaviors of *AvrB*-transformed *P*. *syringae* strains, the
411 ratio of conductivity values measured at 6 hpi and 24 hpi was calculated for each replicated
412 experiment for all modalities that were found to be HR-inducing. This parameter was used as
413 a proxy for HR induction velocity. An analysis of variance of these ratios revealed significant
414 differences among *AvrB*-transformed strains (ANOVA1, $p < 0.05$). DC3000 *AvrB* and M6 *AvrB*
415 proved to be the fastest HR inducers with more than 70% of their total induction already
416 observable at 6 hpi (**Fig. 5**). Yet again, the diversity of behaviors within phylogroups was
417 revealed, even among the three *AvrB*-transformed quasi-clonal strains (**Fig. 5**, post-hoc Dunn's
418 test showed that CC0073 *AvrB* and CC0094 *AvrB* and CC1498 *AvrB* groups differed significantly
419 at $p < 0.05$). Furthermore, 6 hpi/24 hpi-ratios were compared across the different
420 temperatures overall revealing that higher temperatures correlated with faster electrolyte
421 leakage, consistent with the results observed for bacterial *in-vitro* growth (**Supplementary Fig.**
422 **S5**).
423
424 **Whole genome sequences suggest a few candidate genes for temperature-sensitivity.**
425 As we wanted to decipher the origin of sensitivity to the temperature for HR induction, we
426 applied a comparative genomic approach focusing on the three quasi-clonal strains CC0073,

427 CC0094 and CC1498. These strains displayed at least 99.84% homology (ANI calculation).
428 Among the whole set of strains, 286 putative genes were specific to the three CC-strains, and
429 76 were common only to the two warm temperature-dependent ones (CC0094 and CC1498)
430 (**Fig. 6**). By comparing the putative genes present in CC0094 and CC1498 but missing in CC0073
431 (regardless of their presence/absence in the other strains) the list was extended to 173 genes,
432 with 94% of the proteins encoded by these genes unknown (neither the name nor the
433 function) and only 10 putative genes with a known or putative function (**Supplementary Tab.**
434 **S1**).

435 **DISCUSSION**

436

437 **New perspectives on virulence thermoregulation processes.**

438 The diverse behaviors of T3SS efficiency observed in relation to incubation temperature
439 indicate that temperature plays a crucial role in regulating bacterial virulence. This observation
440 is another piece of evidence out of the many reported over the past 30 years regarding the
441 role of temperature in virulence regulation in plant-associated bacteria (reviewed in Smirnova
442 *et al.*, 2001; Velásquez *et al.*, 2018). Our work has presented new examples of relatively warm-
443 temperature dependency for virulence efficiency, consistent with previous findings about gene
444 expression beyond and within the *P. syringae* species complex (Peñaloza-Vázquez *et al.*, 1997;
445 Wei *et al.*, 2008, 2010; Czajkowski *et al.*, 2017; Huot *et al.*, 2017; Krishna *et al.*, 2022).
446 Altogether, these pieces of evidence do not align with the long-standing notion according to
447 which "almost all virulence genes of plant pathogenic bacteria [...] exhibit increased
448 transcription at temperatures well-below the respective growth optima" (Smirnova *et al.*,
449 2001). Such misconception has led some authors to conclude that “the increase of bacterial
450 growth in plants at elevated temperature cannot be explained by variations in intrinsic
451 bacterial growth rate or secretion of effector proteins at different temperatures. A slow HR is
452 also unlikely to be caused by a slow accumulation of bacteria or effector proteins leading to a
453 slower detection by plants” (Wang *et al.*, 2009). Such statements are strongly contradicted by
454 our results, and no longer included in the conclusions of other important and more recent
455 articles that present an implicitly updated perspective with which our work aligns (Huot *et al.*,
456 2017; Velásquez *et al.*, 2018; Tribelli & López, 2022).

457

458 **Effector repertoire role in the lack of HR induction.**

459 Although *AvrB* expression was assessed for all the strains, two of them (J35 *AvrB* and
460 MAFF302273 *AvrB*) were categorized as non-inducers for at least two of the tested
461 temperatures. While HrpZ secretion data *in vitro* confirmed that J35 *AvrB*'s T3SS was unactive,
462 the contrary was demonstrated for MAFF302273 *AvrB*. Consequently, the lack of HR induction
463 could result from the T3SS inactivation in *A. thaliana*, potentially because of a quick PTI onset
464 (Crabill *et al.*, 2010). On the other hand, it could also be a matter of speed of ETI onset, whose
465 rapidity prevents cell death occurrence (Künstler *et al.*, 2016). Otherwise, strain MAFF302273
466 *AvrB* may contain in its repertoire some suppressive effector(s) blocking the ability of AvrB to
467 trigger the HR (Jamir *et al.*, 2004), or some effector(s) targeting a molecular actor involved in
468 both PTI and ETI, or simply blocking the PTI – required in the first place for ETI activation.
469 Consistently we checked for effector repertoire composition for strain MAFF302273 (PsyTEC,
470 Laflamme *et al.*, 2020). To the best of our knowledge, no evidence of direct or indirect
471 antagonism between AvrB and other effectors naturally present was found. However, it is not
472 possible to exclude the occurrence of 'meta-effector' interactions (Kubori *et al.*, 2010; Martel
473 *et al.*, 2022). Overall, the in-depth-study of the effector repertoires of all the strains used in
474 our work could help to explain the differences observed in terms of HR intensity, with one or
475 more effectors that may inhibit HR but also enhance it conversely – as observed for strain
476 CC1498 *AvrB* versus strain CC0094 *AvrB*, for example.
477
478 **Temperature and plant immunity.**
479 Using HR induction as a proxy for T3SS efficiency, we implicitly accounted for plant defense
480 mechanisms that play a role in the response (Künstler *et al.*, 2016). In *A. thaliana*, the role of
481 temperature in plant immunity is more complex than what reported by previous studies. In
482 2009, Wang and colleagues concluded that a mild increase in temperature impaired both PTI

483 and ETI, suggesting a general deficiency in the plant defense system at elevated temperatures
484 (28-30°C) (Wang *et al.*, 2009). Subsequently, a straightforward dichotomy was established: less
485 efficient ETI (effective from 10 to 23°C, with a peak at 18°C) versus more efficient PTI (effective
486 from 23 to 32°C, with a peak at 28°C) as the temperature increases (Cheng *et al.*, 2013). This
487 model was later qualified by the demonstration that, since ETI relies on distinct processes (*i.e.*,
488 virulence suppression and programmed cell death/HR), only HR was inhibited by elevated
489 temperatures as the virulence suppression was maintained (Menna *et al.*, 2015). However,
490 despite their demonstration that ion leakage from *A. thaliana* leaf disks infiltrated with the
491 avirulent DC3000 strain is completely inhibited at 28°C-30°C, our results for this *AvrB*-strain
492 and CC0094 *AvrB* and CC1498 *AvrB* contradict this finding.
493 Temperature variations may affect the kinetics of effector translocation and/or binding to R
494 proteins and hence impact the speed and efficiency of signaling cascades involved in the
495 defense response. Comparison of the ratio of conductivity values measured at 6 hpi and 24 hpi
496 among temperatures for a given HR-inducer strain revealed that the elevation of the
497 temperature led to an acceleration of electrolyte leakage as temperature increased. As this
498 observation was maintained across the strains that induced HR at different temperatures, it is
499 tempting to associate this general effect of accelerated response with the effect of the higher
500 temperature on the plant, and not on the T3SS activation or efficiency. Nevertheless, across all
501 strains, we demonstrated that some were faster than others to induce HR, also indicating some
502 pathosystem-specific behaviors.
503
504 **Temperature and effector secretion properties.**
505 Interestingly, a few examples of temperature-dependency for T3SE secretion have been shown
506 to be 'protein/effector specific' – mentioning some specific secretion properties of AvrB (Van

507 Dijk *et al.*, 1999). Likewise, the two avirulent DC3000 strains with which HR suppression at
508 elevated temperatures was demonstrated carried either the HopZ1a or AvrRpt2 effector
509 (Menna *et al.*, 2015). HopZ1a, AvrRpt2 and AvrB are recognized by the NLRs ZAR1, RPS2 and
510 RPM1, respectively, which are all members of the subgroup of CC-NLRs. The unclear variability
511 of temperature-sensitivity across different NLR subgroups (CC-NLRs versus TIR-NLRs) (Hua,
512 2014; Menna *et al.*, 2015) suggests that sensitivity may not be conserved in all NLRs or CC-
513 NLRs, given their distinct structural and functional properties. In this light, it is reasonable to
514 attribute the differences observed between our work and the one of Menna and colleagues to
515 the different 'ligand-receptor' couples used. Echoing the differences in 'protein/effector
516 specific' secretion efficiency, there are likely to be differences in temperature-sensitivity for
517 effector recognition by R proteins. Overall, we assume that the impact of temperature on T3SS-
518 secretion/ETI/HR-triggering efficiencies can be highly pathosystem-specific. Illustrating this
519 high specificity, DC3000 *AvrB* and M6 *AvrB* displayed a unique behavior among all the tested
520 strains. Being such strong and fast HR inducers probably reflects the fact that they are highly
521 aggressive on *A. thaliana* Col-0 (in their WT version), so the exacerbated response may also be
522 a sign of the global host compatibility between these two strains and the model plant (Preston,
523 2000; Xin & He, 2013).
524
525 **Thermosensing origin and distribution among strains.**
526 We attempted to identify the mechanism(s) that may be responsible for the thermosensitivity
527 at the origin of the different behaviors we observed. Two-component systems such as
528 thermosensor CorRSP responsible for the low-temperature-dependency of coronatin
529 production in *P. syringae* pv. *glycinea* could be involved in the regulation of T3SS-related gene
530 expression in response to temperature (Ullrich *et al.*, 1995). Alternatively, if evidence hints that

531 gene expression is not directly modified by temperature (Puttilli *et al.*, 2022),
532 thermoregulation might act later in the transcription/translation chain, during T3SS assembly,
533 or on translocation efficiency. In addition, the study of potential differences in membrane
534 fluidity between strains is promising. More specifically, membrane fluidity is influenced by
535 functional lipid microdomains ('FMM' or lipid rafts) that are enriched in proteins involved in
536 signal transduction and protein secretion and have the capacity to organize in space and time
537 components of transport machineries (Bramkamp & Lopez, 2015). Likely, T3SS proteins co-
538 localize on lipid rafts to allow their proper assembly, and temperature would impair or favor
539 the process, by changing membrane fluidity.
540 We observed that the behavior of high temperature-preference/dependency is exclusive to
541 strains from phylogroup 2d, whereas the opposite case is specific to strains belonging to
542 phylogroups 1a and 1b. This suggests that temperature responsiveness patterns might vary
543 among strains but remain consistent within the same phylogroup. While the temperature
544 sensitivity feature is widely distributed among the strains, the preference/dependency on low
545 or high temperatures in case of thermosensitivity is conserved within a same phylogroup. This
546 implies that the genes or targets responsible for both processes may be distinct, making their
547 identification more challenging through comparative genomics. Beyond the identification of
548 the mechanisms involved in thermosensitivity, preference/dependency on low or high
549 temperatures could be linked to the evolutionary history of pathogens, which may have been
550 shaped by temperature-related selection pressures. Investigating this question would help
551 shed light on the origin of the phenomenon.
552
553 **Virulence thermoregulation in relation to disease development.**

554 Since the same thermoregulation components may control various virulence factors, one
555 intriguing question is whether the effect of temperature on virulence factors is consistent (i)
556 for a given strain, and (ii) with temperature conditions in which disease occurrence is generally
557 reported. Crossing observations between temperature optimum for virulence and
558 epidemiological data regarding our selected strain revealed a high level of complexity within
559 the *P. syringae* species complex and does not allow us to draw any clearer conclusions.
560 Concerning *P. syringae* pv. *phaseolicola*, the low-temperature-dependency was established for
561 phaseolotoxin production and T6SS regulation, in line with the development of halo blight of
562 bean favored at temperatures below 25°C (Goss, 1940; Nüske & Fritsche, 1989). However,
563 T3SS-related gene expression inhibition has been reported at 18°C (Arvizu-Gómez *et al.*,
564 2013a), and our results indicate that the strain 1448A is thermo-insensitive in its ability to
565 induce HR. Regarding *P. syringae* pv. *actinidiae*, our results confirmed a low-temperature
566 dependency for T3SS efficiency (Puttilli *et al.*, 2022), which is entirely in line with the
567 environmental conditions – in late winter or early spring – under which *P. syringae* pv.
568 *actinidiae* is reported to cause disease or damage in the kiwifruit orchards (Kim *et al.*, 2017;
569 Donati *et al.*, 2020). On the other hand, concerning the strains CC0073 and CC0094 which were
570 isolated from cantaloupe during blight epidemics in southern France in the 90s, the authors
571 have reported that the climatic conditions that favored disease outbreak and development
572 were heavy rainfall associated with a mean minimum temperature below 12-13°C (under
573 which the physiology of cantaloupe comes to a standstill) in 95% of cases, whereas our results
574 demonstrated a major T3SS efficiency at higher temperatures (Morris & Pitrat, 1998; Riffaud,
575 2002; Mention *et al.*, 2004). Finally, strain DC3000 displays a consistent behavior, exhibiting
576 both unaltered T3SS efficiency and coronatine production in response to temperature, at least
577 within the 18°C to 28°C range (Weingart *et al.*, 2004). Its consistency in response to various

578 environmental parameters associated with high reproducibility of data related to it have
579 certainly contributed to making it the model strain it has become. However, this strain was
580 generated in the laboratory as a rifampicin-resistant derivative of the strain DC52, which
581 originated from Guernsey in 1960 (Cuppels, 1986; Xin *et al.*, 2018). Therefore, no conclusive
582 connection could be established between its ecology and its virulence behavior in response to
583 temperature, as this model strain has evolved for many years in laboratories, far from a field
584 context.
585 Another important consideration is that our results highlighted that growth optima – at least
586 *in vitro* – are not correlated with T3SS efficiency. Therefore, providing a definitive answer to
587 the question of whether the temperature conditions that favor virulence (specifically T3SS) are
588 identical to those reported as favorable for disease development is challenging due to both
589 supporting and opposite examples: several traits characterizing phytopathogenic bacteria are
590 thermo-sensitive, and each pathogen is characterized by growth and virulence mechanisms
591 that are activated at precise temperatures, generating a complex scenario in which
592 temperature can alter the outcome of the interaction between plant and bacterium (Tribelli &
593 López, 2022). Consequently, we state that efforts to simplify or generalize the behavior of
594 different strains would not necessarily help our understanding.
595
596 **Interstrain variability.**
597 One important conclusion of our work is the significant variability in behavior among strains,
598 even when closely related at the genomic level (as illustrated with the 3 'CC' strain-quasi-
599 clones). Over the years of research on these issues, examples of such inherent variability in
600 terms of virulence have been largely overlooked, with only a few cases reported in literature,
601 both beyond and within the *P. syringae* species complex (Rohde *et al.*, 1998; Baron *et al.*, 2001;

602 Weingart *et al.*, 2004; Hasegawa *et al.*, 2005). This might be attributed to the commendable
603 aim of simplifying our understanding of the biological models and plant-pathogen interactions
604 under study. However, we emphasize the urgent need to study the diversity among strains,
605 since evidence of their inherent variability has been documented. Although investigating
606 model strains has facilitated the understanding and characterization of intricate molecular
607 mechanisms in plant-pathogen interactions, it is now imperative to consider the full spectrum
608 of *P. syringae* species complex diversity (reported in Berge *et al.*, 2014; Gomila *et al.*, 2017),
609 both within and outside of the agronomic context.

ACKNOWLEDGMENTS

The authors thank Pr. Boris A. Vinatzer, Dr. Perrine Portier, Charlotte Chandeysson and Dr. Marco Scortichini for kindly providing the *P. syringae* strains used in this study. We also thank Pr. Sheng-Yang He for providing the antibody anti-HrpZ. Special thanks to Pr. Roberto Chignola and Dr. Davide Martinetti for their help in analyzing ion-leakage data through statistical approaches. Finally, we also thank the members of the laboratory of plant pathology of the University of Verona for their technical support in conductivity measurements.

618 **REFERENCES**

619

620 **Aguilera S, Alvarez-Morales A, Murillo J, Hernández-Flores JL, Bravo J, De la Torre-Zavala S**.
621 **2017**. Temperature-mediated biosynthesis of the phytotoxin phaseolotoxin by Pseudomonas
622 syringae pv. phaseolicola depends on the autoregulated expression of the phtABC genes (M-
623 J Virolle, Ed.). *PLOS ONE* **12**: e0178441.

624 **Aguilera S, López-López K, Nieto Y, Garcidueñas-Piña R, Hernández-Guzmán G, Hernández-**
625 **Flores JL, Murillo J, Alvarez-Morales A**. **2007**. Functional Characterization of the Gene
626 Cluster from Pseudomonas syringae pv. phaseolicola NPS3121 Involved in Synthesis of
627 Phaseolotoxin. *Journal of Bacteriology* **189**: 2834.

628 **Alfano JR, Bauer DW, Milos TM, Collmer A**. **1996**. Analysis of the role of the Pseudomonas
629 syringae pv. syringae HrpZ harpin in elicitation of the hypersensitive response in tobacco
630 using functionally non-polar hrpZ deletion mutations, truncated HrpZ fragments, and hrmA
631 mutations. *Molecular Microbiology* **19**: 715–728.

632 **Anderson JC, Wan Y, Kim Y-M, Pasa-Tolic L, Metz TO, Peck SC**. **2014**. Decreased abundance
633 of type III secretion system-inducing signals in Arabidopsis mkp1 enhances resistance against
634 Pseudomonas syringae. *Proceedings of the National Academy of Sciences* **111**: 6846–6851.

635 **Arvizu-Gómez JL, Hernández-Morales A, Aguilar JRP, Álvarez-Morales A**. **2013a**.
636 Transcriptional profile of P. syringaepv. phaseolicola NPS3121 at low temperature:
637 Physiology of phytopathogenic bacteria. *BMC Microbiology* **13**: 81.

638 **Arvizu-Gómez JL, Hernández-Morales A, Jofre-Garfias AE, Álvarez-Morales A**. **2013b**.
639 Temperature, the GacS/GacA system, and host metabolites regulate the type VI secretion
640 system of Pseudomonas syringae pv. phaseolicola. *Journal of General Plant Pathology* **79**:
641 194–197.

642 **Balint-Kurti P**. **2019**. The plant hypersensitive response: concepts, control and
643 consequences. *Molecular Plant Pathology* **20**: 1163–1178.
644 **Baltrus DA, McCann HC, Guttman DS**. **2017**. Evolution, genomics and epidemiology of
645 Pseudomonas syringae. *Molecular Plant Pathology* **18**: 152–168.
646 **Baron C, Domke N, Beinhofer M, Hapfelmeier S**. **2001**. Elevated temperature differentially
647 affects virulence, VirB protein accumulation, and T-pilus formation in different
648 Agrobacterium tumefaciens and Agrobacterium vitis strains. *Volume 183, Issue 23, Pages*
649 *6852 - 6861* **183**: 6852–6861.
650 **Bender CL, Alarcón-Chaidez F, Gross DC**. **1999**. Pseudomonas syringae Phytotoxins: Mode
651 of Action, Regulation, and Biosynthesis by Peptide and Polyketide Synthetases . *Microbiology*
652 *and Molecular Biology Reviews* **63**: 266–292.
653 **Berge O, Monteil CL, Bartoli C, Chandeysson C, Guilbaud C, Sands DC, Morris CE**. **2014**. A
654 User's Guide to a Data Base of the Diversity of Pseudomonas syringae and Its Application to
655 Classifying Strains in This Phylogenetic Complex. *PLOS ONE* **9**: e105547.
656 **Boller T, Felix G**. **2009**. A Renaissance of Elicitors: Perception of Microbe-Associated
657 Molecular Patterns and Danger Signals by Pattern-Recognition Receptors. *Annual Review of*
658 *Plant Biology* **60**: 379–406.
659 **Bramkamp M, Lopez D**. **2015**. Exploring the Existence of Lipid Rafts in Bacteria. *Microbiology*
660 *and Molecular Biology Reviews* **79**: 81–100.
661 **Braun Y, Smirnova A V., Weingart H, Schenk A, Ullrich MS**. **2009**. Coronatine gene
662 expression in vitro and in planta, and protein accumulation during temperature downshift in
663 Pseudomonas syringae. *Sensors* **9**: 4272–4285.
664 **Büttner D, He SY**. **2009**. Type III Protein Secretion in Plant Pathogenic Bacteria. *Plant*
665 *Physiology* **150**: 1656–1664.

666 **Cantalapiedra CP, Herṇandez-Plaza A, Letunic I, Bork P, Huerta-Cepas J**. **2021**. eggNOG-
667 mapper v2: Functional Annotation, Orthology Assignments, and Domain Prediction at the
668 Metagenomic Scale. *Molecular Biology and Evolution* **38**: 5825–5829.
669 **Chang JH, Urbach JM, Law TF, Arnold LW, Hu A, Gombar S, Grant SR, Ausubel FM, Dangl JL**.
670 **2005**. A high-throughput, near-saturating screen for type III effector genes from
671 Pseudomonas syringae. *Proceedings of the National Academy of Sciences of the United*
672 *States of America* **102**: 2549–2554.
673 **Cheng C, Gao X, Feng B, Sheen J, Shan L, He P**. **2013**. Plant immune response to pathogens
674 differs with changing temperatures. *Nature Communications* **4**: 2530.
675 **Coll NS, Epple P, Dangl JL**. **2011**. Programmed cell death in the plant immune system. *Cell*
676 *Death & Differentiation* **18**: 1247–1256.
677 **Crabill E, Joe A, Block A, van Rooyen JM, Alfano JR**. **2010**. Plant immunity directly or
678 indirectly restricts the injection of type III effectors by the Pseudomonas syringae type III
679 secretion system. *Plant Physiology* **154**: 233–244.
680 **Cui H, Xiang T, Zhou JM**. **2009**. Plant immunity: a lesson from pathogenic bacterial effector
681 proteins. *Cellular Microbiology* **11**: 1453–1461.
682 **Cunnac S, Lindeberg M, Collmer A**. **2009**. Pseudomonas syringae type III secretion system
683 effectors: repertoires in search of functions. *Current Opinion in Microbiology* **12**: 53–60.
684 **Cuppels DA**. **1986**. Generation and characterization of Tn5 insertion mutations in
685 Pseudomonas syringae pv. tomato. *Applied and Environmental Microbiology* **51**: 323–327.
686 **Czajkowski R, Kaczyńska N, Jafra S, Narajczyk M, Lojkowska E**. **2017**. Temperature-
687 responsive genetic loci in pectinolytic plant pathogenic Dickeya solani. *Plant Pathology* **66**:
688 584–594.
689 **Debener T, Lehnackers H, Arnold M, Dangl JL**. **1991**. Identification and molecular mapping of

690 a single Arabidopsis thaliana locus determining resistance to a phytopathogenic
691 Pseudomonas syringae isolate. *The Plant Journal* **1**: 289–302.
692 **Van Dijk K, Fouts DE, Rehm AH, Hill AR, Collmer A, Alfano JR**. **1999**. The Avr (effector)
693 proteins HrmA (HopPsyA) and AvrPto are secreted in culture from Pseudomonas syringae
694 pathovars via the Hrp (type III) protein secretion system in a temperature- and pH-sensitive
695 manner. *Journal of Bacteriology* **181**: 4790–4797.
696 **Donati I, Cellini A, Sangiorgio D, Vanneste JL, Scortichini M, Balestra GM, Spinelli F**. **2020**.
697 Pseudomonas syringae pv. actinidiae: Ecology, Infection Dynamics and Disease
698 Epidemiology. *Microbial Ecology* **80**: 81–102.
699 **Ferrante P, Scortichini M**. **2010**. Molecular and phenotypic features of Pseudomonas
700 syringae pv. actinidiae isolated during recent epidemics of bacterial canker on yellow
701 kiwifruit (Actinidia chinensis) in central Italy. *Plant Pathology* **59**: 954–962.
702 **Flaugnatti N, Journet L**. **2017**. Identification of Effectors: Precipitation of Supernatant
703 Material. In: 459–464.
704 **Galán JE, Collmer A**. **1999**. Type III Secretion Machines: Bacterial Devices for Protein Delivery
705 into Host Cells. *Science* **284**: 1322–1328.
706 **Gomila M, Busquets A, Mulet M, García-Valdés E, Lalucat J**. **2017**. Clarification of Taxonomic
707 Status within the Pseudomonas syringae Species Group Based on a Phylogenomic Analysis.
708 *Frontiers in Microbiology* **8**: 320397.
709 **Goss RW**. **1940**. The relation of temperature to common and halo blight of beans.
710 *Phytopathology* **30**: 258–264.
711 **Guo M, Tian F, Wamboldt Y, Alfano JR**. **2009**. The Majority of the Type III Effector Inventory
712 of Pseudomonas syringae pv. tomato DC3000 Can Suppress Plant Immunity. *Molecular Plant-*
713 *Microbe Interactions®* **22**: 1069–1080.

714 **Guttman DS, Vinatzer BA, Sarkar SF, Ranall M V., Kettler G, Greenberg JT**. **2002**. A
715 Functional Screen for the Type III (Hrp) Secretome of the Plant Pathogen Pseudomonas
716 syringae. *Science* **295**: 1722–1726.
717 **Hasegawa H, Chatterjee A, Cui Y, Chatterjee AK**. **2005**. Elevated temperature enhances
718 virulence of Erwinia carotovora subsp. carotovora strain EC153 to plants and stimulates
719 production of the quorum sensing signal, N-acyl homoserine lactone, and extracellular
720 proteins. *Volume 71, Issue 8, Pages 4655 - 4663* **71**: 4655–4663.
721 **Hockett KL, Burch AY, Lindow SE**. **2013**. Thermo-Regulation of Genes Mediating Motility and
722 Plant Interactions in Pseudomonas syringae (BA Vinatzer, Ed.). *PLoS ONE* **8**: e59850.
723 **Hua J**. **2014**. Temperature and plant immunity. In: Temperature and Plant Development.
724 Wiley, 163–180.
725 **Hueck CJ**. **1998**. Type III Protein Secretion Systems in Bacterial Pathogens of Animals and
726 Plants. *Microbiology and Molecular Biology Reviews* **62**: 379–433.
727 **Huot B, Castroverde CDM, Velásquez AC, Hubbard E, Pulman JA, Yao J, Childs KL, Tsuda K,**
728 **Montgomery BL, He SY**. **2017**. Dual impact of elevated temperature on plant defence and
729 bacterial virulence in Arabidopsis. *Nature Communications 2017 8:1* **8**: 1–12.
730 **Huynh T V., Dahlbeck D, Staskawicz BJ**. **1989**. Bacterial Blight of Soybean: Regulation of a
731 Pathogen Gene Determining Host Cultivar Specificity. *Science* **245**: 1374–1377.
732 **Imanifard Z, Vandelle E, Bellin D**. **2018**. Measurement of hypersensitive cell death triggered
733 by avirulent bacterial pathogens in Arabidopsis. *Methods in Molecular Biology* **1743**: 39–50.
734 **Innes RW, Bisgrove SR, Smith NM, Bent AF, Staskawicz BJ, Liu Y**. **1993**. Identification of a
735 disease resistance locus in Arabidopsis that is functionally homologous to the RPG1 locus of
736 soybean. *The Plant Journal* **4**: 813–820.
737 **Jain C, Rodriguez-R LM, Phillippy AM, Konstantinidis KT, Aluru S**. **2018**. High throughput ANI

738 analysis of 90K prokaryotic genomes reveals clear species boundaries. *Nature*
739 *Communications* **9**: 5114.
740 **Jamir Y, Guo M, Oh H, Petnicki-Ocwieja T, Chen S, Tang X, Dickman MB, Collmer A, R.**
741 **Alfano J**. **2004**. Identification of Pseudomonas syringae type III effectors that can suppress
742 programmed cell death in plants and yeast. *The Plant Journal* **37**: 554–565.
743 **Jin Q, He S-Y**. **2001**. Role of the Hrp Pilus in Type III Protein Secretion in Pseudomonas
744 syringae. *Science* **294**: 2556–2558.
745 **Jin S, Song YN, Deng WY, Gordon MP, Nester EW**. **1993**. The regulatory VirA protein of
746 Agrobacterium tumefaciens does not function at elevated temperatures. *Journal of*
747 *Bacteriology* **175**: 6830–6835.
748 **Johansson ON, Nilsson AK, Gustavsson MB, Backhaus T, Andersson MX, Ellerström M**.
749 **2015**. A quick and robust method for quantification of the hypersensitive response in plants.
750 *PeerJ* **3**: e1469.
751 **Jones JDG, Dangl JL**. **2006**. The plant immune system. *Nature* **444**: 323–329.
752 **Kim GH, Jung JS, Koh YJ**. **2017**. Occurrence and Epidemics of Bacterial Canker of Kiwifruit in
753 Korea. *The Plant Pathology Journal* **33**: 351–361.
754 **King EO, Ward MK, Raney DE**. **1954**. Two simple media for the demonstration of pyocyanin
755 and fluorescin. *The Journal of Laboratory and Clinical Medicine* **44**: 301–307.
756 **Klinkert B, Narberhaus F**. **2009**. Microbial thermosensors. *Cellular and Molecular Life*
757 *Sciences* **66**: 2661–2676.
758 **Kobayashi T, Kishigami S, Sone M, Inokuchi H, Mogi T, Ito K**. **1997**. Respiratory chain is
759 required to maintain oxidized states of the DsbA-DsbB disulfide bond formation system in
760 aerobically growing Escherichia coli cells. *Proceedings of the National Academy of Sciences of*
761 *the United States of America* **94**: 11857–11862.

762 **Krishna PS, Woodcock SD, Pfeilmeier S, Bornemann S, Zipfel C, Malone JG**. **2022**.
763 Pseudomonas syringae addresses distinct environmental challenges during plant infection
764 through the coordinated deployment of polysaccharides (I Dodd, Ed.). *Journal of*
765 *Experimental Botany* **73**: 2206–2221.
766 **Kubori T, Shinzawa N, Kanuka H, Nagai H**. **2010**. Legionella metaeffector exploits host
767 proteasome to temporally regulate cognate effector. *PLoS Pathogens* **6**: e1001216.
768 **Künstler A, Bacsó R, Gullner G, Hafez YM, Király L**. **2016**. Staying alive – is cell death
769 dispensable for plant disease resistance during the hypersensitive response? *Physiological*
770 *and Molecular Plant Pathology* **93**: 75–84.
771 **Laflamme B, Dillon MM, Martel A, Almeida RND, Desveaux D, Guttman DS**. **2020**. The pan-
772 genome effector-triggered immunity landscape of a host-pathogen interaction. *Science* **367**:
773 763–768.
774 **Lamichhane JR, Messéan A, Morris CE**. **2015**. Insights into epidemiology and control of
775 diseases of annual plants caused by the Pseudomonas syringae species complex. *Journal of*
776 *General Plant Pathology* **81**: 331–350.
777 **Lamichhane JR, Varvaro L, Parisi L, Audergon JM, Morris CE**. **2014**. Disease and frost
778 damage of woody plants caused by pseudomonas syringae: Seeing the forest for the trees.
779 In: Advances in Agronomy. Academic Press Inc., 235–295.
780 **Lee CA**. **1997**. Type III secretion systems: machines to deliver bacterial proteins into
781 eukaryotic cells? *Trends in Microbiology* **5**: 148–156.
782 **Li C-M**. **2002**. The Hrp pilus of Pseudomonas syringae elongates from its tip and acts as a
783 conduit for translocation of the effector protein HrpZ. *The EMBO Journal* **21**: 1909–1915.
784 **Li H, Schenk A, Srivastava A, Zhurina D, Ullrich MS**. **2006**. Thermo-responsive expression
785 and differential secretion of the extracellular enzyme levansucrase in the plant pathogenic

786 bacterium Pseudomonas syringae pv. glycinea. *FEMS Microbiology Letters* **265**: 178–185.

787 **Lindeberg M, Cunnac S, Collmer A**. **2012**. Pseudomonas syringae type III effector

788 repertoires: Last words in endless arguments. *Trends in Microbiology* **20**: 199–208.

789 **Loper JE, Lindow SE**. **1987**. Lack of Evidence for In Situ Fluorescent Pigment Production by

790 Pseudomonas syringae pv. syringae on Bean Leaf Surfaces. *Phytopathology* **77**: 1449.

791 **Mackey D, Holt BF, Wiig A, Dangl JL**. **2002**. RIN4 Interacts with Pseudomonas syringae Type

792 III Effector Molecules and Is Required for RPM1-Mediated Resistance in Arabidopsis. *Cell*

793 **108**: 743–754.

794 **Manni M, Berkeley MR, Seppey M, Simão FA, Zdobnov EM**. **2021**. BUSCO Update: Novel

795 and Streamlined Workflows along with Broader and Deeper Phylogenetic Coverage for

796 Scoring of Eukaryotic, Prokaryotic, and Viral Genomes. *Molecular Biology and Evolution* **38**:

797 4647–4654.

798 **Martel A, Laflamme B, Breit-McNally C, Wang P, Lonjon F, Desveaux D, Guttman DS**. **2022**.

799 Metaeffector interactions modulate the type III effector-triggered immunity load of

800 Pseudomonas syringae. *PLOS Pathogens* **18**: e1010541.

801 **Melotto M, Kunkel BN**. **2013**. Virulence strategies of plant pathogenic bacteria. In: The

802 Prokaryotes: Prokaryotic Physiology and Biochemistry. Springer-Verlag Berlin Heidelberg,

803 61–82.

804 **Menna A, Nguyen D, Guttman DS, Desveaux D**. **2015**. Elevated temperature differentially

805 influences effector-triggered immunity outputs in Arabidopsis. *Frontiers in Plant Science* **6**:

806 1–7.

807 **Mention P, Lavigne D, Leix-Henry F, Bouchu S, Morris CE, Prior P, Pitrat M, Mercy L, Dours**.

808 **2004**. Bactériose du melon: acquis et perspectives. *PHM Revue Horticole*: 22–26.

809 **Monteil CL, Yahara K, Studholme DJ, Mageiros L, Méric G, Swingle B, Morris CE, Vinatzer**

810 **BA, Sheppard SK**. **2016**. Population-genomic insights into emergence, crop adaptation and
811 dissemination of Pseudomonas syringae pathogens. *Microbial genomics* **2**: e000089.
812 **Monteiro F, Nishimura MT**. **2018**. Structural, Functional, and Genomic Diversity of Plant NLR
813 Proteins: An Evolved Resource for Rational Engineering of Plant Immunity. *Annual Review of*
814 *Phytopathology* **56**: 243–267.
815 **Morris CE, Glaux C, Latour X, Gardan L, Samson R, Pitrat M**. **2000**. The Relationship of Host
816 Range, Physiology, and Genotype to Virulence on Cantaloupe in Pseudomonas syringae from
817 Cantaloupe Blight Epidemics in France.
818 **Morris CE, Lamichhane JR, Nikolić I, Stanković S, Moury B**. **2019**. The overlapping
819 continuum of host range among strains in the Pseudomonas syringae complex.
820 *Phytopathology Research* **1**: 4.
821 **Morris CE, Pitrat M**. **1998**. La bactériose du melon : connaissances acquises et travaux en
822 cours. *PHM Revue Horticole*: 44–47.
823 **Morris CE, Sands DC, Vanneste JL, Montarry J, Oakley B, Guilbaud C, Glaux C**. **2010**.
824 Inferring the Evolutionary History of the Plant Pathogen Pseudomonas syringae from Its
825 Biogeography in Headwaters of Rivers in North America, Europe, and New Zealand (S
826 Lindow, Ed.). *mBio* **1**.
827 **Morris CE, Sands DC, Vinatzer BA, Glaux C, Guilbaud C, Buffière A, Yan S, Dominguez H,**
828 **Thompson BM**. **2008**. The life history of the plant pathogen Pseudomonas syringae is linked
829 to the water cycle. *The ISME Journal* **2**: 321–334.
830 **Mudgett MB**. **2005**. New insights to the function of phytopathogenic bacterial type III
831 effectors in plants. *Annual Review of Plant Biology* **56**: 509–531.
832 **Mudgett MB, Staskawicz BJ**. **1998**. Protein signaling via type III secretion pathways in
833 phytopathogenic bacteria. *Current Opinion in Microbiology* **1**: 109–115.

834 **Ngou BPM, Ahn HK, Ding P, Jones JDG**. **2021**. Mutual potentiation of plant immunity by cell-
835 surface and intracellular receptors. *Nature 2021 592:7852* **592**: 110–115.
836 **Nüske J, Fritsche W**. **1989**. Phaseolotoxin production by Pseudomonas syringae pv.
837 phaseolicola: The influence of temperature. *Journal of Basic Microbiology* **29**: 441–447.
838 **Palmer DA, Bender CL**. **1993**. Effects of Environmental and Nutritional Factors on Production
839 of the Polyketide Phytotoxin Coronatine by Pseudomonas syringae pv. Glycinea. *Applied and*
840 *Environmental Microbiology* **59**: 1619–1626.
841 **Peñaloza-Vázquez A, Kidambi SP, Chakrabarty AM, Bender CL**. **1997**. Characterization of the
842 alginate biosynthetic gene cluster in Pseudomonas syringae pv. syringae. *Journal of*
843 *Bacteriology* **179**: 4464–4472.
844 **Preston GM**. **2000**. Pseudomonas syringae pv. tomato : the right pathogen, of the right
845 plant, at the right time. *Molecular Plant Pathology* **1**: 263–275.
846 **Puttilli MR, Danzi D, Correia C, Brandi J, Cecconi D, Manfredi M, Marengo E, Santos C,**
847 **Spinelli F, Polverari A, *et al.* 2022**. Plant Signals Anticipate the Induction of the Type III
848 Secretion System in Pseudomonas syringae pv. actinidiae , Facilitating Efficient Temperature-
849 Dependent Effector Translocation . *Microbiology Spectrum* **10**.
850 **Riffaud C**. **2002**. La bactériose du melon : écologie et stratégies de lutte contre Pseudomonas
851 syringae pv.aptata.
852 **Rohde BH, Pohlack B, Ullrich MS**. **1998**. Occurrence of thermoregulation of genes involved
853 in coronatine biosynthesis among variousPseudomonas syringae strains. *Journal of Basic*
854 *Microbiology* **38**: 41–50.
855 **Roine E, Wei W, Yuan J, Nurmiaho-Lassila EL, Kalkkinen N, Romantschuk M, He SY**. **1997**.
856 Hrp pilus: An hrp-dependent bacterial surface appendage produced by Pseudomonas
857 syringae pv. tomato DC3000. *Proceedings of the National Academy of Sciences of the United*

858 *States of America* **94**: 3459–3464.

859 **Ruiz-Bedoya T, Wang PW, Desveaux D, Guttman DS**. **2023**. Cooperative virulence via the
860 collective action of secreted pathogen effectors. *Nature Microbiology* **8**: 640–650.

861 **Sawada H, Suzuki F, Matsuda I, Saitou N**. **1999**. Phylogenetic analysis of Pseudomonas
862 syringae pathovars suggests the horizontal gene transfer of argK and the evolutionary
863 stability of hrp gene cluster. *Journal of Molecular Evolution* **49**: 627–644.

864 **Scalschi L, Fernández-Crespo E, Pitarch-Marin M, Llorens E, González-Hernández AI,**
865 **Camañes G, Vicedo B, García-Agustín P**. **2022**. Response of Tomato-Pseudomonas
866 Pathosystem to Mild Heat Stress. *Horticulturae* **8**: 174.

867 **Seemann T**. **2014**. Prokka: Rapid prokaryotic genome annotation. *Bioinformatics* **30**: 2068–
868 2069.

869 **Sharma A, Gupta AK, Devi B**. **2023**. Current trends in management of bacterial pathogens
870 infecting plants. *Antonie van Leeuwenhoek* **116**: 303–326.

871 **Smirnova A, Li H, Weingart H, Aufhammer S, Burse A, Finis K, Schenk A, Ullrich MS**. **2001**.
872 Thermoregulated expression of virulence factors in plant-associated bacteria. *Archives of*
873 *Microbiology* **176**: 393–399.

874 **Stevens RB**. **1960**. JG Horsfall and AE Dimond, eds. In: Horsfall JG, Dimond AE, eds. Plant
875 Pathology, an Advanced Treatise, Vol. 3. Academic Press, NY, 357–429.

876 **Takikawa Y, Serizawa S, Ichikawa T, Tsuyumu S, Goto M**. **1989**. Pseudomonas syringae pv.
877 actinidiae pv. nov.: The causal bacterium of canker of kiwifruit in Japan. *Japanese Journal of*
878 *Phytopathology* **55**: 437–444.

879 **Taylor JD, Teverson DM, Allen DJ, Pastor-Corrales MA**. **1996**. Identification and origin of
880 races of Pseudomonas syringae pv. phaseolicola from Africa and other bean growing areas.
881 *Plant Pathology* **45**: 469–478.

882 **Thomma BPHJ, Nürnberger T, Joosten MHAJ**. **2011**. Of PAMPs and Effectors: The Blurred
883 PTI-ETI Dichotomy. *The Plant Cell* **23**: 4–15.
884 **Di Tommaso P, Chatzou M, Floden EW, Barja PP, Palumbo E, Notredame C**. **2017**. Nextflow
885 enables reproducible computational workflows. *Nature Biotechnology* **35**: 316–319.
886 **Tonkin-Hill G, MacAlasdair N, Ruis C, Weimann A, Horesh G, Lees JA, Gladstone RA, Lo S,**
887 **Beaudoin C, Floto RA, *et al.* 2020**. Producing polished prokaryotic pangenomes with the
888 Panaroo pipeline. *Genome Biology* **21**: 1–21.
889 **Tribelli PM, López NI**. **2022**. Insights into the temperature responses of Pseudomonas
890 species in beneficial and pathogenic host interactions. *Applied Microbiology and*
891 *Biotechnology* **106**: 7699–7709.
892 **Ullrich M, Penaloza-Vazquez A, Bailey AM, Bender CL**. **1995**. A modified two-component
893 regulatory system is involved in temperature- dependent biosynthesis of the Pseudomonas
894 syringae phytotoxin coronatine. *Journal of Bacteriology* **177**: 6160–6169.
895 **Ullrich MS, Schergaut M, Boch J, Ullrich B**. **2000**. Temperature-responsive genetic loci in the
896 plant pathogen Pseudomonas syringae pv. glycinea. *Microbiology* **146**: 2457–2468.
897 **Velásquez AC, Castroverde CDM, He SY**. **2018**. Plant–Pathogen Warfare under Changing
898 Climate Conditions. *Current Biology* **28**: R619–R634.
899 **Wang Y, Bao Z, Zhu Y, Hua J**. **2009**. Analysis of Temperature Modulation of Plant Defense
900 Against Biotrophic Microbes. *Molecular Plant-Microbe Interactions®* **22**: 498–506.
901 **Wei M, KeisukeTakeshima, Yokoyama T, Minamisawa K, Mitsui H, Itakura M, Kaneko T,**
902 **Tabata S, Saeki K, Omori H, *et al.* 2010**. Temperature-dependent expression of type III
903 secretion system genes and its regulation in bradyrhizobium japonicum. *Molecular Plant-*
904 *Microbe Interactions* **23**: 628–637.
905 **Wei M, Yokoyama T, Minamisawa K, Mitsui H, Itakura M, Kaneko T, Tabata S, Saeki K,**

906 **Omori H, Tajima S, *et al.* 2008**. Soybean Seed Extracts Preferentially Express Genomic Loci of
907 Bradyrhizobium japonicum in the Initial Interaction with Soybean, Glycine max (L.) Merr.
908 *DNA Research* **15**: 201–214.
909 **Weingart H, Stubner S, Schenk A, Ullrich MS**. **2004**. Impact of temperature on in planta
910 expression of genes involved in synthesis of the Pseudomonas syringae phytotoxin
911 coronatine. *Molecular Plant-Microbe Interactions* **17**: 1095–1102.
912 **Whalen MC, Innes RW, Bent AF, Staskawicz BJ**. **1991**. Identification of Pseudomonas
913 syringae pathogens of Arabidopsis and a bacterial locus determining avirulence on both
914 Arabidopsis and soybean. *The Plant Cell* **3**: 49.
915 **Xin XF, He SY**. **2013**. Pseudomonas syringae pv. tomato DC3000: A model pathogen for
916 probing disease susceptibility and hormone signaling in plants. *Annual Review of*
917 *Phytopathology* **51**: 473–498.
918 **Xin X-F, Kvitko B, He SY**. **2018**. Pseudomonas syringae: what it takes to be a pathogen.
919 *Nature Reviews Microbiology* **16**: 316–328.
920 **Xin X-F, Nomura K, Aung K, Velásquez AC, Yao J, Boutrot F, Chang JH, Zipfel C, He SY**. **2016**.
921 Bacteria establish an aqueous living space in plants crucial for virulence. *Nature* **539**: 524–
922 529.
923 **Yuan M, Jiang Z, Bi G, Nomura K, Liu M, Wang Y, Cai B, Zhou JM, He SY, Xin XF**. **2021**.
924 Pattern-recognition receptors are required for NLR-mediated plant immunity. *Nature 2021*
925 *592:7852* **592**: 105–109.
926

Table 1: Set of selected *P. syringae* strains.

PHYLOGROUP	STRAIN	FULL NAME	ALIAS IN COLLECTIONS	ISOLATION SOURCE	COUNTRY	YEAR	REFERENCE
1a	DC3000	*P. syringae* pv. *tomato*	CFBP 7438, ICMP 18429	*Solanum lycopersicum*	United-Kingdom	1960	Cuppels, 1986
	M6	*P. syringae* pv. *maculicola*	CFBP 4314, NCPPB 1766, LMG 5560	*Brassica oleracea* var. Botrytis	United-Kingdom	1965	Debener *et al.* , 1991
	T1	*P. syringae* pv. *tomato*	-	*Solanum lycopersicum*	Canada	1986	Whalen *et al.* , 1991
	LAB0041	*P. syringae*	-	Epilithic biofilm	France	2009	Berge *et al.* , 2014
1b	J35	*P. syringae* pv. *actinidiae*	CFBP 4909, ICMP 9617, NCPPB 3739	*Actinidia deliciosa* cv. Hayward	Japan	1984	Takikawa *et al.* , 1989
	CRA-FRU 8.43	*P. syringae* pv. *actinidiae*	-	*Actinidia chinensis* cv. Hort16	Italy	2008	Ferrante & Scortichini, 2010
	USA007	*P. syringae*	CFBP 8574	Creek water	United States of America	2007	Morris *et al.* , 2010
2d	CC0073	*P. syringae* pv. *aptata*	CFBP 5430	*Cucumis melo*	France	1997	Morris *et al.* , 2000
	CC0094	*P. syringae* pv. *aptata*	CFBP 8529	*Cucumis melo*	France	1997	Morris *et al.* , 2000
	CC1498	*P. syringae*	-	Snowfall	France	2006	Morris *et al.* , 2008
	B728a	*P. syringae* pv. *syringae*	CFBP 8502, ICMP 18427, NCPPB 4487, LMG 26717	*Phaseolus vulgaris*	United States of America	1987	Loper & Lindow, 1987
	MAFF302273	*P. syringae* pv. *aceris*	CFBP 2339, ICMP 2802, NCPPB 958, LMG 2106	*Acer* sp.	United States of America	1939	Sawada *et al.* , 1999
3a	1448A	*P. syringae* pv. *phaseolicola*	CFBP 7087, NCPPB 4478	*Phaseolus vulgaris*	Ethiopia	1985	Taylor *et al.* , 1996

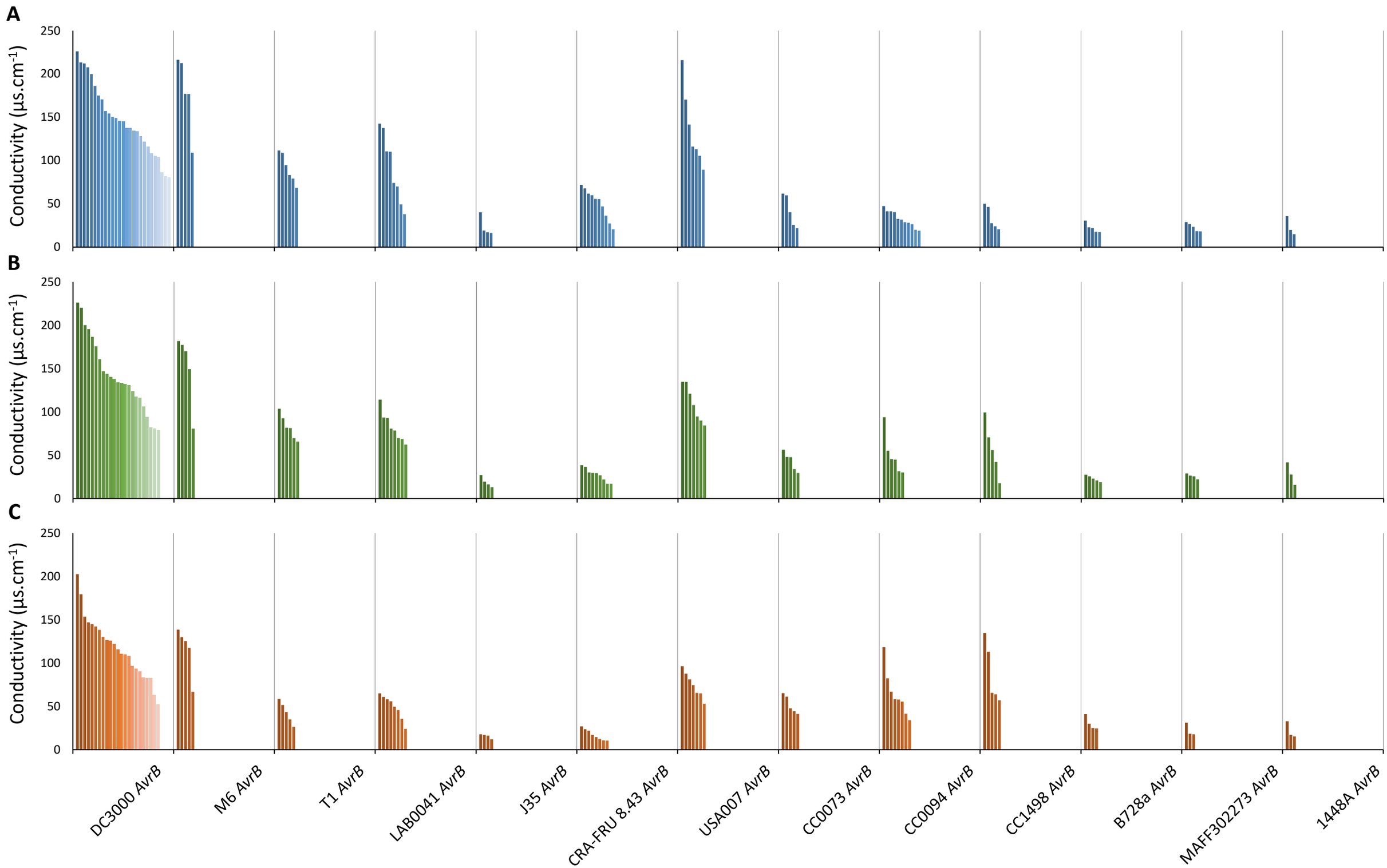

Figure 1: Variability in the increase of conductivity measured at 24 hours post-inoculation (hpi) over the replicated experiments performed for each *AvrB*-carrying strain, at 18°C (A), 24°C (B) and 28°C (C). Bars represent the mean increase in conductivity for each of the independent biological replicates ($3 \leq n \leq 27$). Values are sorted from left to right in a descending order.

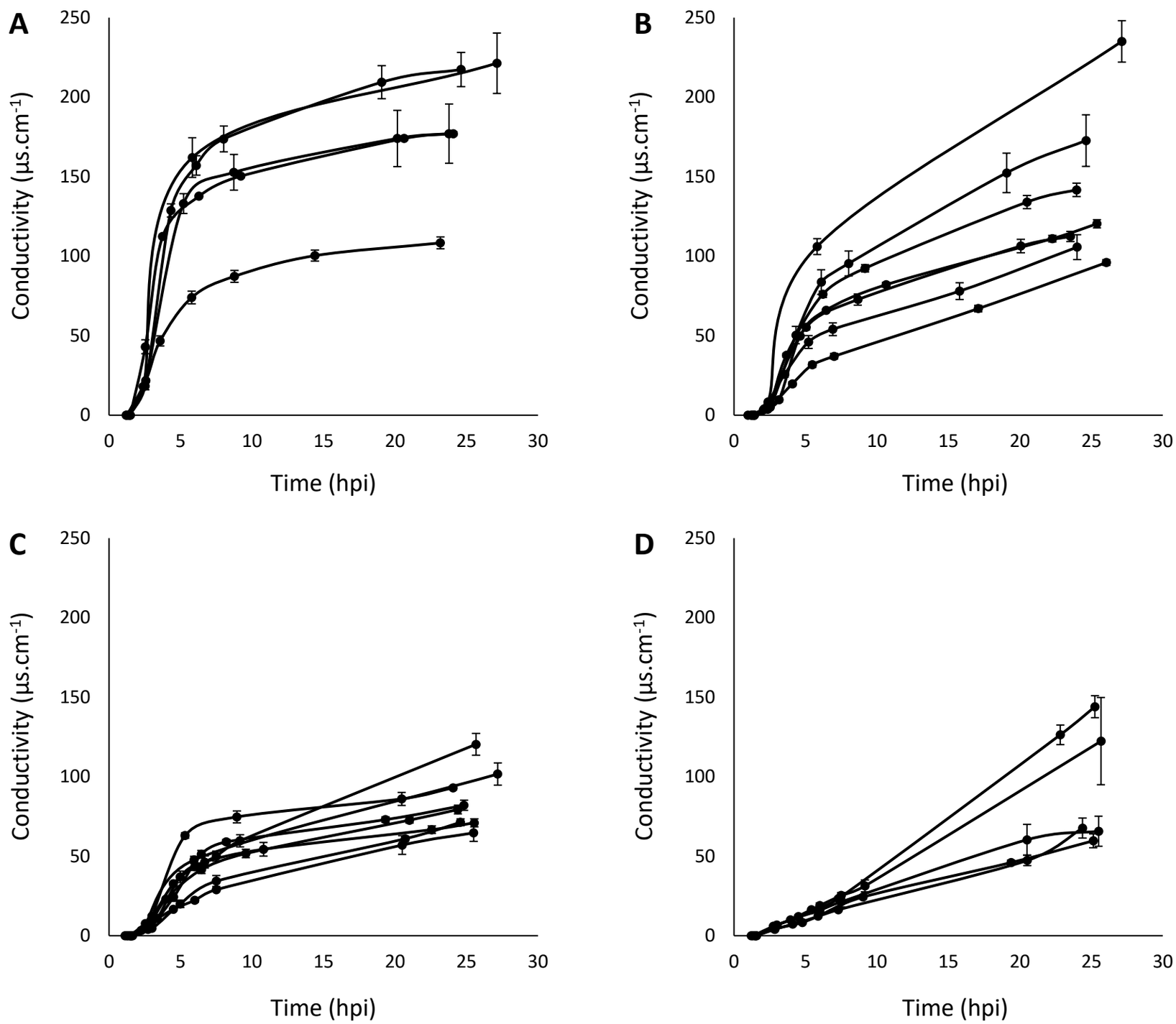

Figure 2: Electrolyte leakage curves obtained post-infiltration for strain M6 *AvrB* at 18°C (A), USA007 *AvrB* at 18°C (B), LAB0041 *AvrB* at 24°C (C) and CC1498 *AvrB* at 28°C (D). Each curve represents the mean increase in conductivity measured over time for one independent biological replicate performed with three technical replicates each. Error bars represent standard error.

Table 2: Statistics associated with linear mixed-effects models fit to ion leakage experiment results. The effect of strains was calculated for each mutant bacterium at each temperature by comparing with the results obtained for the mock treatment (MgCl2 10mM). Significant values of the estimate parameter ($p < 0.05$, in bold) are associated with HR inducing conditions. The temperature effect was evaluated for each AvrB-carrying strain, inducing HR at least at two temperatures (non-inducer strains are highlighted in grey), comparing the electrolyte leakage curves obtained at these different temperatures. Strains insensitive to the temperature ($p > 0.05$) are highlighted in green, strains leading to minor conductivity levels as the temperature increases (negative estimate, $p < 0.05$) are highlighted in blue, and strains displaying a warm-dependency (positive estimate, $p < 0.05$) are highlighted in red. The number of replicated experiments for each modality (strain x temperature condition) varied from 3 up to 27.

PHYLOGROUP	STRAIN	INDUCER AT A GIVEN TEMPERATURE						TEMPERATURE EFFECT	
		18°C		24°C		28°C			
		Estimate	*p-value*	*Estimate*	*p-value*	*Estimate*	*p-value*	*p-value*	*Estimate*
1a	DC3000	69.97	**2.00E-16**	73.12	**1.25E-15**	65.27	**8.46E-15**	8.02E-01	-0.19
	M6	95.14	**2.00E-16**	89.06	**5.35E-16**	73.05	**1.59E-14**	1.95E-01	-2.07
	T1	28.98	**2.00E-16**	29.07	**2.00E-16**	13.45	**2.81E-08**	**1.42E-02**	**-1.26**
	LAB0041	31.36	**4.24E-11**	29.56	**2.00E-16**	16.83	**2.83E-09**	5.17E-02	-1.22
1b	J35	3.35	5.43E-02	0.18	9.19E-01	-1.27	4.46E-01	NA	
	CRA-FRU 8.43	14.09	**4.69E-11**	4.97	**4.33E-04**	0.97	4.45E-01	**3.80E-03**	**-1.28**
	USA007	52.24	**2.00E-16**	46.69	**8.58E-16**	34.15	**2.26E-12**	**3.35E-02**	**-1.70**
2d	CC0073	15.22	**5.97E-07**	15.28	**7.62E-07**	19.77	**3.42E-09**	3.55E-01	0.63
	CC0094	6.86	**6.44E-08**	9.72	**2.61E-06**	14.49	**8.91E-08**	**9.76E-04**	**0.97**
	CC1498	7.89	**4.96E-06**	12.69	**2.24E-05**	19.96	**1.52E-08**	**2.58E-02**	**1.36**
	B728a	3.12	**2.08E-02**	2.22	1.61E-01	4.75	**8.07E-03**	**4.27E-02**	**0.37**
	MAFF302273	3.17	**1.73E-02**	2.88	9.68E-02	1.78	3.77E-01	NA	
3a	1448A	5.14	**1.07E-02**	6.73	**9.73E-03**	2.46	2.41E-01	6.41E-01	0.53

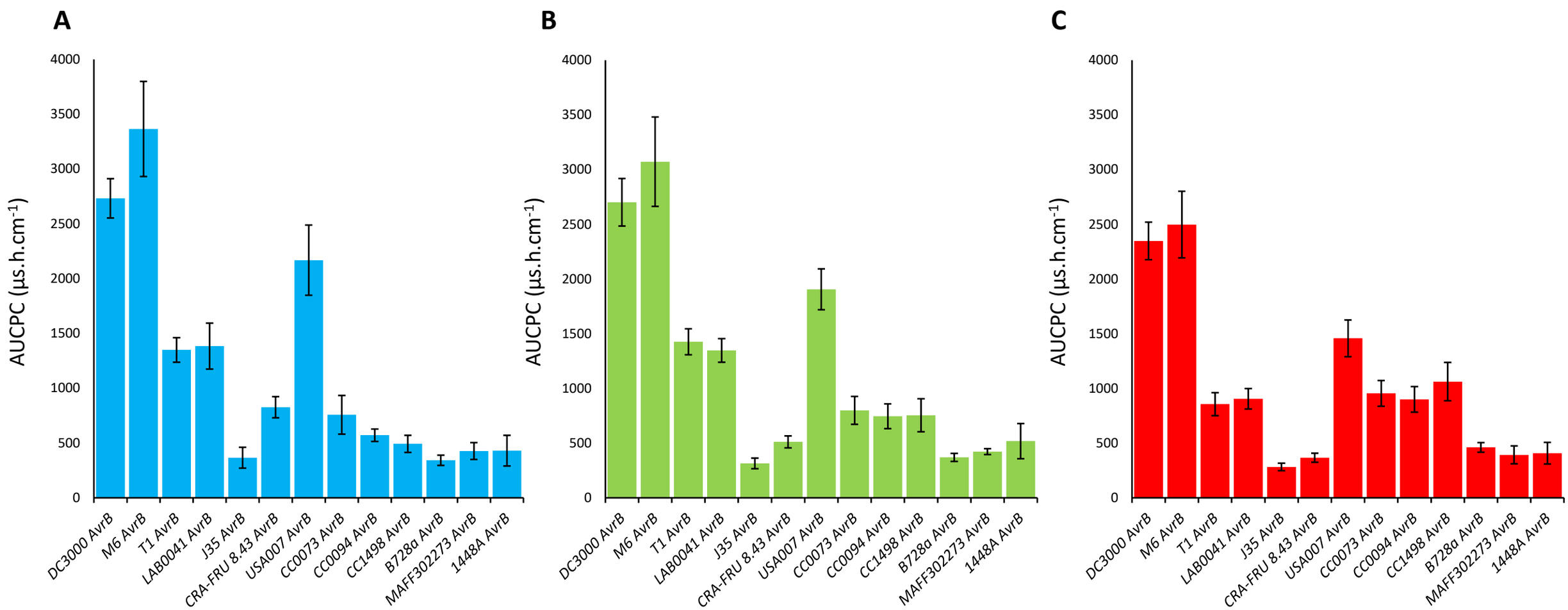

Figure 3: Mean area under conductivity progress curve (AUCPC) calculations for all the replicated experiments (3 ≤ n ≤ 27) of each *AvrB*-carrying strain at 18°C (A), 24°C (B) and 28°C (C). Error bars represent standard error.

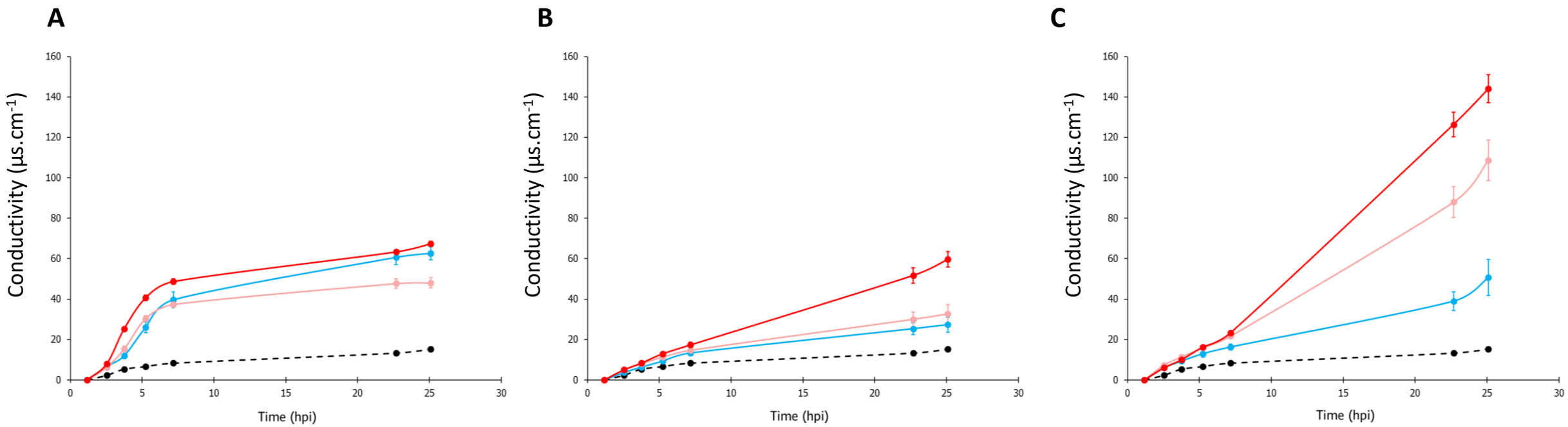

Figure 4: Electrolyte leakage curves over time obtained post-infiltration for CC0073 *AvrB* (A), CC0094 *AvrB* (B) and CC1498 *AvrB* (C) at 18°C (blue), 24°C (pink) and 28°C (red) and of the mock treatment ($MgCl_2$ 10mM, black dotted line) at 24°C. Data represent one single representative biological replicate with all strains and temperature conditions evaluated simultaneously with three technical replicates each. Error bars represent standard error.

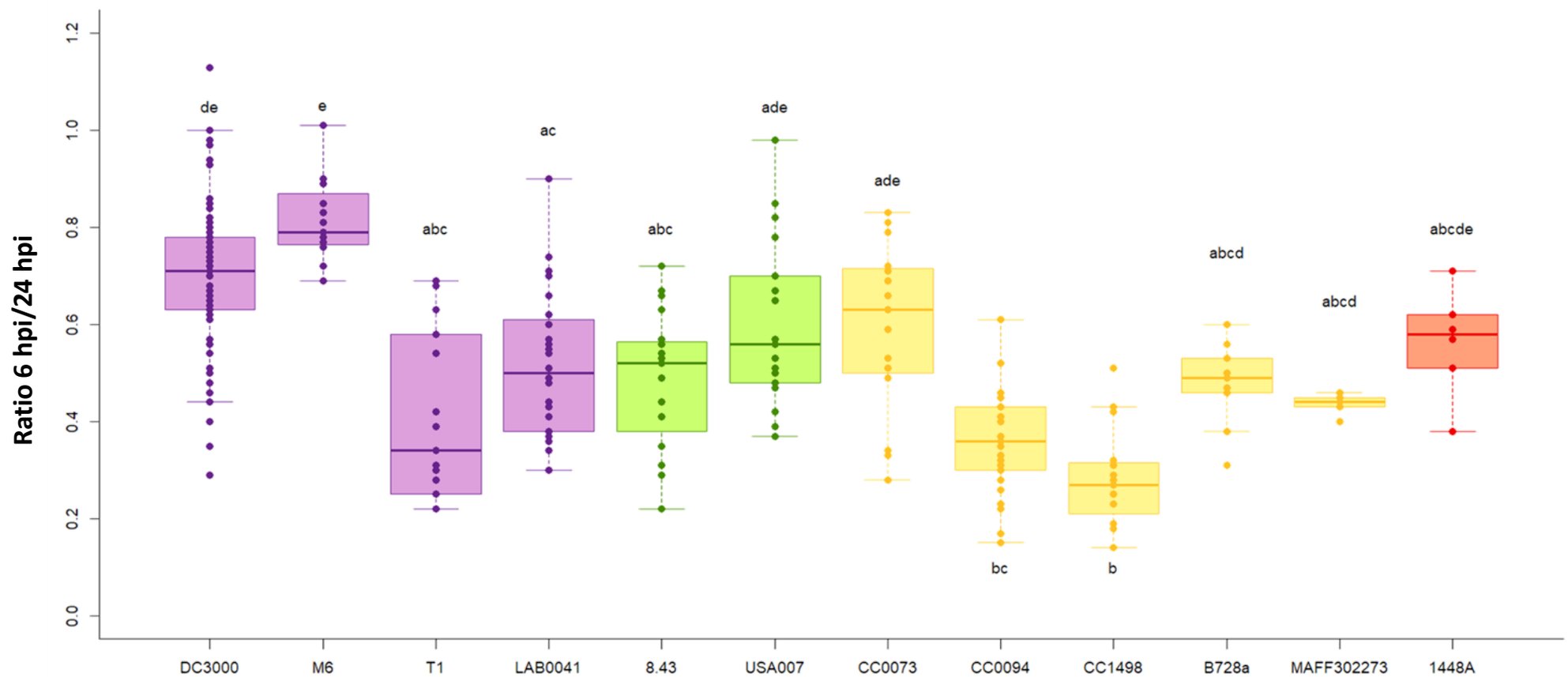

Figure 5: Estimation of velocity of HR induction. The proxy for velocity was calculated as the ratio of conductivity increase measured at 6 hpi and 24 hpi for each *AvrB*-carrying strain inducing HR at least at one temperature condition. Strains are sorted by phylogroup from left to right, PG1a (purple), PG1b (green), PG2d (yellow), PG3a (red). Boxes were calculated from 5 up to 73 replicated experiments per strain (single dots). Boxes associated with different letters represent significantly different means ($p < 0.05$, according to a Kruskal-Wallis test followed by post-hoc Dunn's test).

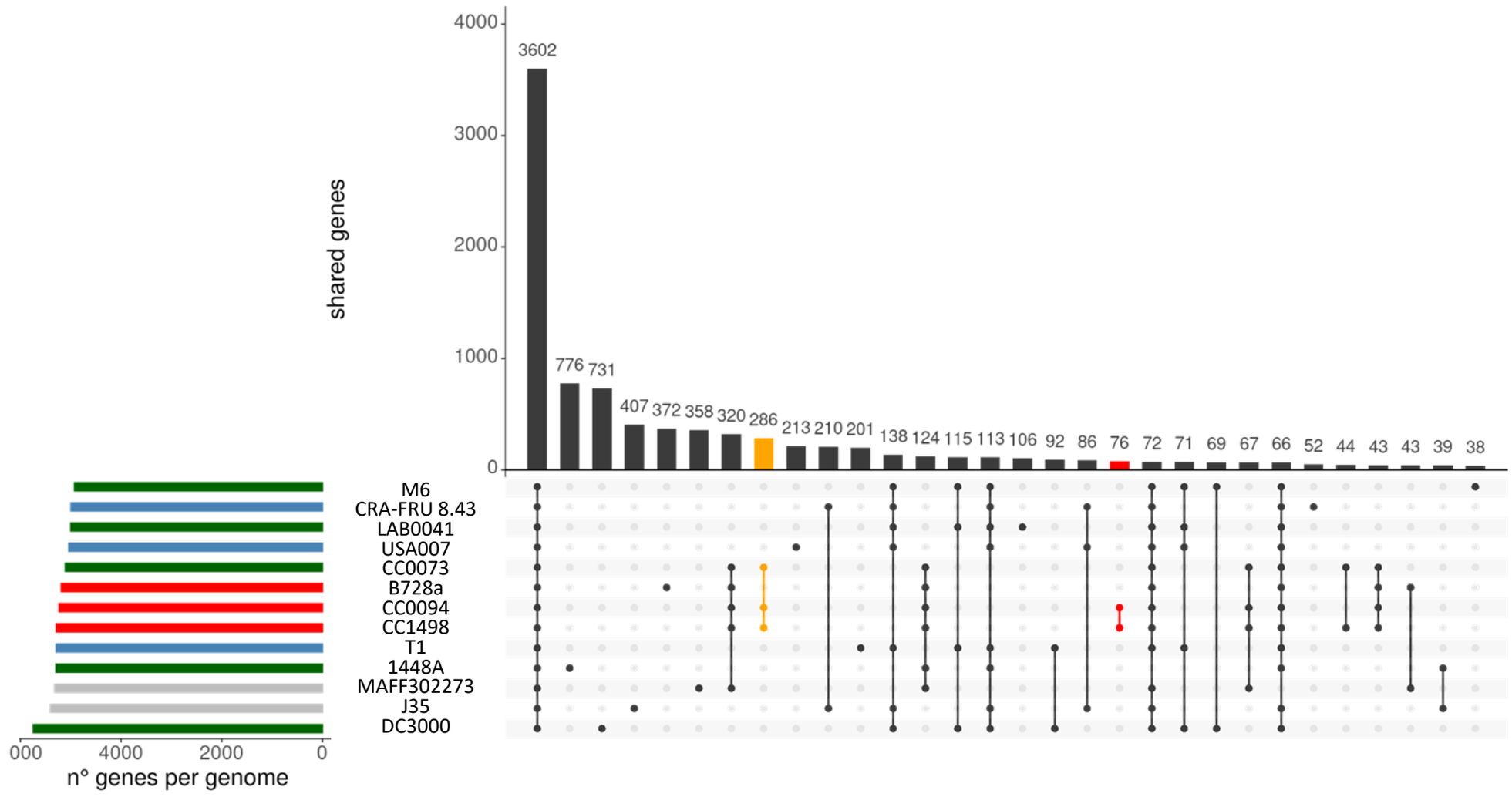

Figure 6: Comparative genomics performed for the 13 strains characterized in ion leakage experiments. Vertical bars correspond to the number of genes shared by groups of strains or exclusively present in single strains (group/strain-specific genes). Horizontal color bars represent the type of behavior of each strain in response to temperature, as identified in Tab. 2. Common putative genes specific to the 3 quasi-clonal strains CC0073, CC0094 and CC1498 are in yellow, common putative genes specific to CC0094 and CC1498 are in red.